

Fundamental Limits of Spectrum Sharing for NOMA-Based Cooperative Relaying Under a Peak Interference Constraint

Vaibhav Kumar, *Student Member, IEEE*, Barry Cardiff, *Senior Member, IEEE*,
and Mark F. Flanagan, *Senior Member, IEEE*

Abstract

Non-orthogonal multiple access (NOMA) and spectrum sharing (SS) are two emerging multiple access technologies for efficient spectrum utilization in future wireless communications standards. In this paper, we present the performance analysis of a NOMA-based cooperative relaying system (CRS) in an underlay spectrum sharing scenario, considering a peak interference constraint (PIC), where the peak interference inflicted by the secondary (unlicensed) network on the primary-user (licensed) receiver (PU-Rx) should be less than a predetermined threshold. In the proposed system the relay and the secondary-user receiver (SU-Rx) are equipped with multiple receive antennas and apply selection combining (SC), where the antenna with highest instantaneous signal-to-noise ratio (SNR) is selected, and maximal-ratio combining (MRC), for signal reception. Closed-form expressions are derived for the average achievable rate and outage probabilities for SS-based CRS-NOMA. These results show that for large values of peak interference power, the SS-based CRS-NOMA outperforms the CRS with conventional orthogonal multiple access (OMA) in terms of spectral efficiency. The effect of the interference channel on the system performance is also discussed, and in particular, it is shown that the interference channel between the secondary-user transmitter (SU-Tx) and the PU-Rx has a more severe effect on the average achievable rate as compared

The authors are with School of Electrical and Electronic Engineering, University College Dublin, Ireland (e-mail: vaibhav.kumar@ucdconnect.ie, barry.cardiff@ucd.ie, mark.flanagan@ieee.org).

Part of the content of this paper appeared in the Proc. of the IEEE Global Communications Conference (GLOBECOM'18) - NOMAT5G Workshop, Abu Dhabi, 09-13 Dec. 2018.

This publication has emanated from research conducted with the financial support of Science Foundation Ireland (SFI) and is co-funded under the European Regional Development Fund under Grant Number 13/RC/2077.

to that between the relay and the PU-Rx. A close agreement between the analytical and numerical results confirm the correctness of our rate and outage analysis.

I. Introduction

With the proliferation of wireless communication technologies, services and applications, one of the major challenges for the successful implementation of future wireless communications standards is that of supporting large-scale heterogeneous data traffic. NOMA has recently been recognized as a promising multiple-access technology for long-term evolution advanced (LTE-A), 5G and beyond-5G wireless networks [1]–[3]. Many variants of NOMA have been suggested in the literature, e.g., power-domain NOMA [4], sparse code multiple access (SCMA), interleaved division multiple access (IDMA), low-density spreading (LDS), pattern division multiple access (PDMA) [5] and lattice partition multiple access (LPMA) [6]. Among all these variants, power-domain NOMA has gained widespread popularity because of its implementation-friendly transceiver architecture (we will refer to power-domain NOMA simply as ‘NOMA’ throughout this paper). It can accommodate several users within the same orthogonal resource block (time, frequency and/or spreading code) via multiplexing them in the power domain at the transmitter and using successive interference cancellation (SIC) at the receiver to remove the messages intended for other users. In the case of NOMA, users with poor channel conditions have a larger share of transmission power, unlike the conventional OMA where more power is allocated to users with strong channel conditions (also known as the water-filling strategy) [3].

Cognitive radio (CR) is another potential solution to the spectrum scarcity problem, as it can enhance the radio spectrum utilization efficiency via SS. The three main SS paradigms include *underlay*, *overlay* and *interweave* approaches [7]. In an underlay SS system, secondary/unlicensed users (SUs) operate in a frequency band originally owned by a PU such that the interference caused by the SUs on the primary network is lower than a predefined threshold, frequently referred to as the *interference temperature* [8]. Therefore, no limit is directly imposed on the power transmitted from a SU-Tx; it is sufficient that the interference caused at the PU receiver (PU-Rx) is below the threshold. In a fading channel, the secondary network may take advantage of this fact by opportunistically transmitting at high power when the interference channel between SU-Tx and PU-Rx is in a deep fade. A closed-form expression for the secondary channel capacity under a constraint on the (peak or average) interference inflicted on the PU-Rx was presented in [9] for different channel models including additive white Gaussian noise (AWGN), log-normal shadowing, Rayleigh fading and Nakagami-m fading.

The interference from the PU transmitter (PU-Tx) to the SU-Rx, also termed as the primary-to-secondary interference, was not considered in [9] and hence the results derived serve as an upper-bound on the average achievable rate for the secondary network.

A very promising application of NOMA for power-domain multiplexed transmission using a cooperative relaying system (CRS-NOMA) was proposed in [10], where the source was able to deliver two different symbols to the destination in two time slots with the help of a relay. It was shown in [10] that CRS-NOMA outperforms the conventional OMA based decode-and-forward cooperative relaying system in terms of the average achievable rate in the case of Rayleigh fading channels. The performance superiority of CRS-NOMA in Rician fading was shown in [11].

The integration of NOMA into a spectrum sharing system can further enhance the spectral efficiency of a wireless network. Different models of spectrum sharing NOMA networks, including underlay NOMA, overlay NOMA and cognitive NOMA, were discussed in [12], and it was shown that cooperative relaying can improve reception reliability. As such, cooperative spectrum sharing NOMA networks have lower outage probability compared to their non-cooperative counterparts. Interference management, energy efficiency, multi-carrier cognitive NOMA, cognitive MIMO-NOMA, relay selection/user scheduling, physical-layer security and full-duplex cognitive NOMA were recognized as some of the future challenges in the integration of CR and NOMA technologies in [12]. System design guidelines for full-duplex NOMA in CR networks was provided in [13], and it was noted that the performance of half-duplex CR-NOMA systems becomes strictly restricted because of the co-channel interference and the interference constraint imposed by the primary network. A novel secondary NOMA-relay-assisted spectrum sharing scheme was proposed in [14], where first the quality-of-service (QoS) of the PU was guaranteed using MRC and then the sum-rate of the SUs was maximized. In [15], a cooperative NOMA-based spectrum sharing system was proposed, where the primary network shared the spectrum with the secondary network in exchange for a form of cooperation where the secondary transmitter transmitted the primary user's message as well as its own message using NOMA. Using the tools of stochastic geometry, the outage performance of a NOMA-based large scale underlay CR with randomly deployed users was characterized in [16]. The energy efficiency optimization of a multiuser multiple-input single-output (MISO) NOMA system using CR-inspired NOMA subject to an individual QoS constraint for each primary user was discussed in [17]. The outage performance of a two-user decode-and-forward underlay CR-NOMA system was studied in [18]. It was assumed in [18] that the transmission from the relay does not cause any interference to the primary receiver, and also that there is no interference from the primary transmitter to the secondary receivers. The

outage performance of a similar system with imperfect channel state information was presented in [19], where the interference from the relay to the primary network and the interference from the primary network to the secondary network was also considered.

In this paper, we analyze the performance of the CRS-NOMA in an underlay SS scenario, where the power transmitted from the SU-Tx and from the relay are constrained by placing a limit on the peak interference power received at the PU-Rx. For clarity of exposition, no other constraint on the transmit power is imposed. While in practice the transmit power from the SU-Tx or the relay is limited by hardware capabilities and other health-related safety considerations, the rates derived in this paper serve as an upper-bound on the capacity of the SS-based CRS-NOMA under a peak interference power constraint. The main contributions of this paper are summarized as follows:

- First, we derive analytical closed-form expressions for the average achievable sum-rate and outage probability for the CRS-NOMA in an underlay SS scenario for the case where all nodes are equipped with a single antenna.
- Next, we derive closed-form expressions for the average achievable sum-rate and outage probability for the SS-based CRS-NOMA in a scenario where the relay and the SU-Rx are equipped with multiple receive antennas. We consider two different diversity combining schemes at both relay and destination for signal reception – SC and MRC. In the case of SC, the closed-form expressions are represented using elementary functions, whereas for MRC, the expressions are represented using Meijer’s G-function, the EGBMGF, the Gauss hypergeometric function and some elementary functions.
- We compare the average achievable sum-rate of the SS-based CRS-NOMA with that of the SS-based CRS-OMA and show that the former outperforms the latter for large values of peak interference power at the PU-Rx.
- We also present the asymptotic analysis of the outage probability for SS-based CRS-NOMA.

The rest of this paper is organized as follows: Section II describes the system model for SS-based CRS-NOMA. In Section III, we present a detailed analysis of the average achievable sum-rate and outage probability of the system considering that all nodes are equipped with a single antenna. In Section IV, we present the analysis for the CRS-NOMA where the relay and the SU-Rx are equipped with multiple receive antennas and SC is used for combining the received signals at the respective nodes. Section V deals with the case when both relay and SU-Rx are equipped with multiple receive antennas and MRC is employed for diversity combining. Results

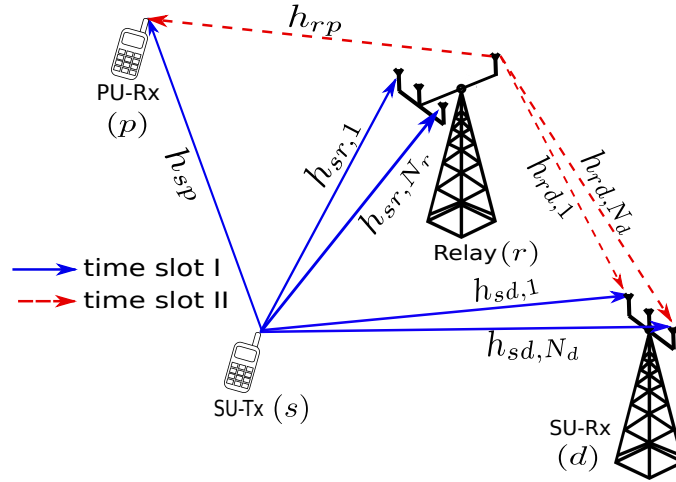


Fig. 1: System model for CRS-NOMA with underlay spectrum sharing.

and discussion are presented in Section VI and finally, conclusions are drawn in Section VII.

II. System Model

Consider an SS-based CRS-NOMA system as shown in Fig. 1, which consists of a SU-Tx s , a relay r , a SU-Rx d and a PU-Rx p . The SU-Tx s is equipped with a single transmit antenna and the PU-Rx p is equipped with a single receive antenna. The relay r is equipped with $N_r (\geq 1)$ receive antennas and a single transmit antenna, while the SU-Rx d is equipped with $N_d (\geq 1)$ receive antennas. It is assumed that all nodes are operating in the half-duplex mode and all wireless links are independent and Rayleigh distributed. The channel coefficient between the SU-Tx and the i^{th} receive antenna of the relay ($1 \leq i \leq N_r$) is denoted by $h_{sr,i}$ and has a mean-square value Ω_{sr} for all i , while that between the SU-Tx and the j^{th} antenna of the SU-Rx ($1 \leq j \leq N_d$) is denoted by $h_{sd,j}$ and has a mean-square value Ω_{sd} for all j . The channel coefficient between the transmit antenna of the relay and the j^{th} antenna of the SU-Rx is denoted by $h_{rd,j}$ and has a mean-square value Ω_{rd} for all j . Moreover, the channel coefficient between the SU-Tx and the PU-Rx is denoted by h_{sp} and has a mean-square value Ω_{sp} , while that between the relay and the PU-Rx is denoted by h_{rp} and has a mean-square value Ω_{rp} . Furthermore, it is assumed that the channels between the SU-Tx and the SU-Rx are on average weaker than those between the SU-Tx and the relay, i.e., $\Omega_{sd} < \Omega_{sr}$.

We assume that perfect knowledge of h_{sp} and h_{rp} are available at the SU-Tx and the relay, respectively; this helps in determining the transmit power so that the received interference power at the PU-Rx never exceeds the tolerance limit Q . Also, the knowledge of Ω_{sr} and Ω_{sd}

is assumed to be available at the SU-Tx. Moreover, we assume that perfect knowledge of $\{h_{sr,i}\}$ is available at the relay, and perfect knowledge of $\{h_{sd,j}\}$ and $\{h_{rd,k}\}$ is available at the SU-Rx. It is important to note that these CSI requirements are similar to those assumed in [9] and [10].

In the CRS-NOMA scheme with spectrum sharing, the SU-Tx broadcasts $\sqrt{a_1 P_s(h_{sp})}s_1 + \sqrt{a_2 P_s(h_{sp})}s_2$ to both relay and SU-Rx, where s_1 and s_2 are the data-bearing constellation symbols which are multiplexed in the power domain ($\mathbb{E}\{|s_i|^2\} = 1$ for $i = 1, 2$). $P_s(h_{sp})$ is the power transmitted from the SU-Tx and in general is a mapping from the fading coefficient h_{sp} to the set of non-negative real numbers \mathbb{R}_+ such that the instantaneous interference at the PU-Rx does not exceed a predetermined value (interference temperature). Moreover, a_1 and a_2 are power weighting coefficients satisfying the constraints $a_1 + a_2 = 1$ and $a_1 > a_2$. After receiving the signal from the SU-Tx, the SU-Rx decodes symbol s_1 treating the interference from s_2 as additional noise, while the relay first decodes symbol s_1 and then applies SIC to decode s_2 . In the second time slot, the SU-Tx remains silent and only the relay transmits its estimate of symbol s_2 , denoted as \hat{s}_2 , to the SU-Rx with power $P_r(h_{rp})$ which in general is a mapping from the fading coefficient h_{rp} to \mathbb{R}_+ such that the instantaneous interference at the primary receiver does not exceed the predetermined threshold. In this manner, two different symbols are delivered to the secondary receiver in two time slots.

In contrast to this, in the conventional OMA with underlay spectrum sharing scheme, the SU-Tx broadcasts symbol s_1 with power $P_s(h_{sp})$ in the first time slot and the relay retransmits its estimate of symbol s_1 , denoted by \hat{s}_1 , to the SU-Rx with power $P_r(h_{rp})$ in the second time slot. The SU-Rx then combines both copies of symbol s_1 and in this manner only a single symbol is delivered to the SU-Rx in two time slots.

III. Performance Analysis: Single Antenna Case

In this section we present the average achievable sum-rate and outage probability analysis for the SS-based CRS-NOMA under peak interference constraint for the case when $N_r = N_d = 1$. Note that while the more general case ($N_r \geq 1, N_d \geq 1$) will be considered later, for this special case the derived expressions for the average achievable rate and outage probability have a particularly simple form which is not trivial to deduce from the solution to the general case; thus it is worthwhile to consider the single antenna case separately.

Here we denote the channel coefficients for s-r, s-d, r-d, s-p and r-p links by h_{sr} , h_{sd} , h_{rd} , h_{sp} and h_{rp} respectively. The signal received at the relay (resp. SU-Rx and PU-Rx) in the first

time slot is given by

$$y_{s\ell} = h_{s\ell} \left(\sqrt{a_1 P_s(h_{sp})} s_1 + \sqrt{a_2 P_s(h_{sp})} s_2 \right) + n_{s\ell},$$

where $\ell = r$ (resp. $\ell = d$ and $\ell = p$) and, $n_{s\ell}$ is complex additive white Gaussian noise (AWGN) with zero mean and unit variance. The received instantaneous signal-to-interference-plus-noise ratio (SINR) at the relay for decoding symbol s_1 and the received instantaneous SNR for decoding symbol s_2 (assuming symbol s_1 is decoded correctly) are, respectively,

$$\gamma_{sr}^{(1)} = \frac{\lambda_{sr} a_1 P_s(h_{sp})}{\lambda_{sr} a_2 P_s(h_{sp}) + 1}, \quad \gamma_{sr}^{(2)} = \lambda_{sr} a_2 P_s(h_{sp}),$$

where $\lambda_{sr} \triangleq |h_{sr}|^2$. Similarly, the received instantaneous SINR at the SU-Rx for decoding symbol s_1 is given by

$$\gamma_{sd} = \frac{\lambda_{sd} a_1 P_s(h_{sp})}{\lambda_{sd} a_2 P_s(h_{sp}) + 1},$$

where $\lambda_{sd} \triangleq |h_{sd}|^2$. In the next time slot, the relay transmits its estimate of symbol s_2 , denoted by \hat{s}_2 , to the SU-Rx with power $P_r(h_{rp})$. The signal received at the SU-Rx (resp. PU-Rx) in the second time slot is given by

$$y_{r\sigma} = h_{r\sigma} \sqrt{P_r(h_{rp})} \hat{s}_2 + n_{r\sigma},$$

where $\sigma = d$ (resp. $\sigma = p$) and $n_{r\sigma}$ is complex AWGN with zero mean and unit variance. The received SNR at the SU-Rx for decoding symbol s_2 is given by

$$\gamma_{rd} = \lambda_{rd} P_r(h_{rp}),$$

where $\lambda_{rd} \triangleq |h_{rd}|^2$. Since the symbol s_1 should be decoded correctly at the SU-Rx as well as at the relay for SIC, while satisfying the interference constraint at the PU-Rx, the average achievable rate for symbol s_1 is given by (c.f. [10, Eqn. (8)], [9, Eqn. (1), Eqn. (22)])

$$\bar{C}_{s_1} = \max_{P_s(h_{sp}) \geq 0} \int_{|h_{sp}|} \int_{|h_{sr}|} \int_{|h_{sd}|} 0.5 \log_2 \left(1 + \min \left\{ \gamma_{sr}^{(1)}, \gamma_{sd} \right\} \right) g_1(|h_{sp}|) g_2(|h_{sr}|) g_3(|h_{sd}|) d|h_{sp}| \times d|h_{sr}| d|h_{sd}|, \quad (1)$$

$$\text{s.t.} \quad \lambda_{sp} P_s(h_{sp}) \leq Q, \quad (2)$$

where the maximization in (1) is performed over all possible transmit power mappings $P_s(h_{sp}) > 0$ and Q is the peak interference power that the PU-Rx can tolerate from the secondary network; and $g_1(|h_{sp}|)$, $g_2(|h_{sr}|)$ and $g_3(|h_{sd}|)$ denote the probability density functions (PDFs) of $|h_{sp}|$, $|h_{sr}|$ and $|h_{sd}|$ respectively. Assuming no other limitation on the power transmitted from the SU-Tx,

the optimal transmit power $P_s^*(h_{sp})$ which maximizes the achievable rate is given by Q/λ_{sp} .

Hence, the average achievable rate for symbol s_1 is given by

$$\begin{aligned}\bar{C}_{s_1} &= 0.5 \int_{|h_{sp}|} \int_{|h_{sr}|} \int_{|h_{sd}|} \log_2 \left(1 + \frac{\frac{\min\{\lambda_{sr}, \lambda_{sd}\}}{\lambda_{sp}} Q a_1}{\frac{\min\{\lambda_{sr}, \lambda_{sd}\}}{\lambda_{sp}} Q a_2 + 1} \right) g_1(|h_{sp}|) g_2(|h_{sr}|) g_3(|h_{sd}|) d|h_{sp}| \\ &\quad \times d|h_{sr}| d|h_{sd}| \\ &= \frac{1}{2} \left[\int_0^\infty \log_2(1+Qx) f_X(x) dx - \int_0^\infty \log_2(1+Qa_2x) f_X(x) dx \right],\end{aligned}\quad (3)$$

where $X \triangleq \min\{\lambda_{sr}, \lambda_{sd}\}/\lambda_{sp}$ and $f_W(\cdot)$ denotes the PDF of the random variable W .

Theorem 1. A closed-form expression for the average achievable rate for the symbol s_1 is given by

$$\bar{C}_{s_1} = 0.5 \left[\frac{Q \log_2 \left(\frac{Q}{\phi \Omega_{sp}} \right)}{Q - \phi \Omega_{sp}} - \frac{a_2 Q \log_2 \left(\frac{a_2 Q}{\phi \Omega_{sp}} \right)}{a_2 Q - \phi \Omega_{sp}} \right], \quad (4)$$

where $\phi \triangleq (1/\Omega_{sr}) + (1/\Omega_{sd})$.

Proof: See Appendix A.

Similarly, the average achievable rate for symbol s_2 is given by (c.f. [10, Eqn. (9)], [9, Eqn. (1), Eqn. (22)])

$$\begin{aligned}\bar{C}_{s_2} &= \max_{\substack{P_s(h_{sp}) \geq 0 \\ P_r(h_{rp}) \geq 0}} \int_{|h_{sp}|} \int_{|h_{rp}|} \int_{|h_{sr}|} \int_{|h_{rd}|} 0.5 \log_2 \left(1 + \min \left\{ \gamma_{sr}^{(2)}, \gamma_{rd} \right\} \right) g_1(|h_{sp}|) g_2(|h_{sr}|) g_4(|h_{rp}|) g_5(|h_{rd}|) \\ &\quad \times d|h_{sp}| d|h_{sr}| d|h_{rp}| d|h_{rd}|,\end{aligned}\quad (5)$$

$$\text{s.t. } \lambda_{sp} P_s(h_{sp}) \leq Q, \quad (6)$$

$$\lambda_{rp} P_r(h_{rp}) \leq Q, \quad (7)$$

where $g_4(|h_{rp}|)$ and $g_5(|h_{rd}|)$ denote the PDFs of $|h_{rp}|$ and $|h_{rd}|$, respectively. Assuming no other limitation on the power transmitted from the relay, the optimal transmit power $P_r^*(h_{rp})$ which maximizes the achievable rate is given by Q/λ_{rp} . Therefore, the average achievable rate for symbol s_2 is given by

$$\begin{aligned}\bar{C}_{s_2} &= \int_{|h_{sp}|} \int_{|h_{rp}|} \int_{|h_{sr}|} \int_{|h_{rd}|} 0.5 \log_2 \left(1 + \min \left\{ \frac{\lambda_{sr} a_2}{\lambda_{sp}}, \frac{\lambda_{rd}}{\lambda_{rp}} \right\} Q \right) g_1(|h_{sp}|) g_2(|h_{sr}|) g_4(|h_{rp}|) g_5(|h_{rd}|) \\ &\quad \times d|h_{sp}| d|h_{sr}| d|h_{rp}| d|h_{rd}| \\ &= \frac{1}{2} \int_0^\infty \log_2(1+Qx) f_Y(x) dx = \frac{0.5Q}{\ln(2)} \int_0^\infty \frac{1 - F_Y(x)}{1+Qx} dx,\end{aligned}\quad (8)$$

where $Y \triangleq \min\{\lambda_{sr}a_2/\lambda_{sp}, \lambda_{rd}/\lambda_{rp}\}$ and $F_{\mathcal{W}}(\cdot)$ denotes the cumulative distribution function (CDF) of the random variable \mathcal{W} .

Theorem 2. A closed-form expression for the average achievable rate for the symbol s_2 is given by

$$\bar{C}_{s_2} = \frac{0.5 a_2 \Omega_{rd} \Omega_{sr} Q \left[\Omega_{rp} \Omega_{sp} \log_2 \left(\frac{a_2 \Omega_{rp} \Omega_{sr}}{\Omega_{rd} \Omega_{sp}} \right) + a_2 \Omega_{rp} \Omega_{sr} Q \log_2 \left(\frac{\Omega_{rd} Q}{\Omega_{rp}} \right) - \Omega_{rd} \Omega_{sp} Q \log_2 \left(\frac{a_2 \Omega_{sr} Q}{\Omega_{sp}} \right) \right]}{(\Omega_{rd} \Omega_{sp} - a_2 \Omega_{rp} \Omega_{sr})(\Omega_{rd} Q - \Omega_{rp})(\Omega_{sp} - a_2 \Omega_{sr} Q)}. \quad (9)$$

Proof: See Appendix B.

Using (4) and (9), the average achievable sum-rate for the CRS-NOMA system is given as

$$\bar{C}_{\text{sum}} = \bar{C}_{s_1} + \bar{C}_{s_2}. \quad (10)$$

In theory the system with single antenna (at the relay and SU-Rx) are special case when the relay and SU-Rx are equipped with multiple receive antennas, however, the analysis leads to simple closed-form expressions for the average achievable sum-rate and outage probability, and these expressions are not trivial to obtain from the generalized case of multiple antennas.

For the case of OMA, the signal received at the relay (resp. SU-Rx and PU-Rx) in the first time slot is given by

$$y_{s\ell, \text{OMA}} = h_{s\ell} \sqrt{P_s(h_{sp})} s_1 + n_{s\ell},$$

where $\ell = r$ (resp. $\ell = d$ and $\ell = p$). In the second time slot, the relay transmits its estimate of s_1 , denoted by \hat{s}_1 , to the SU-Rx. The signal received at the SU-Rx (resp. PU-Rx) in the second time slot is given by

$$y_{r\sigma, \text{OMA}} = h_{r\sigma} \sqrt{P_r(h_{rp})} \hat{s}_1 + n_{r\sigma},$$

where $\sigma = d$ (resp. $\sigma = p$). Following the same peak interference constraint as in the case of NOMA, the average achievable rate for the SS-based CRS-OMA is given by

$$\bar{C}_{\text{OMA}} = 0.5 \mathbb{E}_Z [\log_2(1 + QZ)], \quad (11)$$

where¹ $Z \triangleq \min \left\{ \frac{\lambda_{sr}}{\lambda_{sp}}, \frac{\lambda_{sd}}{\lambda_{sp}} + \frac{\lambda_{rd}}{\lambda_{rp}} \right\}$ and $\mathbb{E}_{\mathcal{W}}[\cdot]$ denotes the expectation with respect to the random variable \mathcal{W} .

¹Here we assume that the SU-Rx applies MRC on the two copies of s_1 .

Outage probability for CRS-NOMA: We define \mathcal{O}_1 as the outage event for symbol s_1 , i.e., the event when either the relay or the SU-Rx fails to decode s_1 successfully. Hence the outage probability for symbol s_1 is given by

$$\begin{aligned} \Pr(\mathcal{O}_1) &= \Pr(C_{s_1} < R_1) = \Pr\left[0.5 \log_2 \left(1 + \frac{\alpha_1 QX}{\alpha_2 QX + 1}\right) < R_1\right] \\ &= \Pr(X < \Theta_1) = \int_0^{\Theta_1} f_X(x) dx = \int_0^{\Theta_1} \frac{\phi \Omega_{sp} dx}{(1 + \phi \Omega_{sp} x)^2} = \frac{\phi \Omega_{sp} \Theta_1}{1 + \phi \Omega_{sp} \Theta_1}, \end{aligned} \quad (12)$$

where C_{s_1} is the instantaneous achievable rate for symbol s_1 , R_1 is the target data rate for symbol s_1 , $\epsilon_1 = 2^{2R_1} - 1$ and $\Theta_1 = \frac{\epsilon_1}{Q(\alpha_1 - \epsilon_1 \alpha_2)}$. The integration above is solved using (33) and [20, Eqn. (3.194-1), p. 315]. The system design must ensure that $\alpha_1 > \epsilon_1 \alpha_2$, otherwise the outage probability for symbol s_1 will always be 1 as noted in [21]. Next, we define \mathcal{O}_2 as the outage event for symbol s_2 . This outage event can be decomposed as the union of the following disjoint events: (i) symbol s_1 cannot be successfully decoded at the relay; (ii) symbol s_1 is successfully decoded at the relay, but symbol s_2 cannot be successfully decoded at the relay; and (iii) both symbols are successfully decoded at the relay, but symbol s_2 cannot be successfully decoded at the SU-Rx. Therefore, the outage probability for the symbol s_2 may be expressed as

$$\begin{aligned} \Pr(\mathcal{O}_2) &= \begin{cases} \Pr\left(\frac{\lambda_{sr}}{\lambda_{sp}} < \Theta_1\right) + \Pr\left(\frac{\lambda_{sr}}{\lambda_{sp}} \geq \Theta_1, \frac{\lambda_{sr}}{\lambda_{sp}} < \Theta_2\right) + \Pr\left(\frac{\lambda_{sr}}{\lambda_{sp}} \geq \Theta_2, \frac{\lambda_{rd}}{\lambda_{rp}} < \frac{\epsilon_2}{Q}\right); & \text{if } \Theta_1 < \Theta_2 \\ \Pr\left(\frac{\lambda_{sr}}{\lambda_{sp}} < \Theta_1\right) + \Pr\left(\frac{\lambda_{sr}}{\lambda_{sp}} \geq \Theta_1, \frac{\lambda_{rd}}{\lambda_{rp}} < \frac{\epsilon_2}{Q}\right); & \text{otherwise} \end{cases} \\ &= F_{\frac{\lambda_{sr}}{\lambda_{sp}}}(\Theta) + F_{\frac{\lambda_{rd}}{\lambda_{rp}}}\left(\frac{\epsilon_2}{Q}\right) - F_{\frac{\lambda_{sr}}{\lambda_{sp}}}(\Theta) F_{\frac{\lambda_{rd}}{\lambda_{rp}}}\left(\frac{\epsilon_2}{Q}\right), \end{aligned} \quad (13)$$

where R_2 is the target data rate for symbol s_2 , $\epsilon_2 = 2^{2R_2} - 1$, $\Theta_2 = \frac{\epsilon_2}{\alpha_2 Q}$ and $\Theta = \max(\Theta_1, \Theta_2)$. Using (35), the closed-form expression for the outage probability of symbol s_2 is given by

$$\Pr(\mathcal{O}_2) = \frac{\Omega_{sp} \Theta}{\Omega_{sr} + \Omega_{sp} \Theta} + \frac{\epsilon_2 \Omega_{rp}}{Q \Omega_{rd} + \epsilon_2 \Omega_{rp}} - \frac{\Omega_{sp} \Omega_{rp} \epsilon_2 \Theta}{(\Omega_{sr} + \Omega_{sp} \Theta)(\Omega_{rd} Q + \Omega_{rp} \epsilon_2)}. \quad (14)$$

On the other hand, for the SS-based CRS-OMA system, the outage probability is given by

$$\Pr(\mathcal{O}_{OMA}) = \Pr(Z < \epsilon_1).$$

Asymptotic behavior of CRS-NOMA

Using (12), for large values of Q we have

$$\Pr(\mathcal{O}_1) = \frac{\phi \Omega_{sp} \epsilon_1}{Q(\alpha_1 - \epsilon_1 \alpha_2) + \phi \Omega_{sp} \epsilon_1} = \frac{1}{1 + \beta Q} = \frac{1}{\beta Q} \sum_{k=0}^{\infty} (-1)^k \left(\frac{1}{\beta Q}\right)^k = \frac{1}{\beta Q} + \mathbf{o}(Q^{-2}),$$

where $\beta \triangleq (\alpha_1 - \epsilon_1 \alpha_2) / (\phi \Omega_{sp} \epsilon_1)$ and $\mathbf{O}(\cdot)$ is the Landau symbol. The above relation holds good for $\beta Q > 1$. Therefore, it is clear that for the single-antenna case, the outage probability for s_1 decays as Q^{-1} for large Q . Similarly, for large values of Q

$$F_{\lambda_{sp}}^{\lambda_{sr}}(\Theta) = \frac{\Omega_{sp} \Theta}{\Omega_{sr} + \Omega_{sp} \Theta} = \frac{\Omega_{sp} \beta^\dagger}{\Omega_{sr} Q} \sum_{k=0}^{\infty} (-1)^k \left(\frac{\Omega_{sp} \beta^\dagger}{\Omega_{sr} Q} \right)^k = \frac{\Omega_{sp} \beta^\dagger}{\Omega_{sr} Q} + \mathbf{O}(Q^{-2}),$$

where $\beta^\dagger \triangleq \max \left\{ \frac{\epsilon_1}{\alpha_1 - \epsilon_1 \alpha_2}, \frac{\epsilon_2}{\alpha_2} \right\}$. Hence, $F_{\lambda_{sp}}^{\lambda_{sr}}(\Theta)$ decays as Q^{-1} for large Q values. Analogously, it can be shown that $F_{\lambda_{rp}}^{\lambda_{rd}} \left(\frac{\epsilon_2}{Q} \right)$ decays as Q^{-1} and $F_{\lambda_{sp}}^{\lambda_{sr}}(\Theta) F_{\lambda_{rp}}^{\lambda_{rd}} \left(\frac{\epsilon_2}{Q} \right)$ decays as Q^{-2} . Therefore, using (13), it is clear that the outage probability for s_2 decays as Q^{-1} for large values of Q .

IV. Performance Analysis: Selection Combining

In this section, we generalize the results obtained in the previous section for the case when $N_r \geq 1$, $N_d \geq 1$ and selection combining (SC), i.e., selection of the antenna with highest instantaneous SNR, is used for reception at both relay and SU-Rx. In the first time-slot, the received instantaneous SINR at the relay for decoding symbol s_1 and the instantaneous SNR for decoding symbol s_2 (assuming the symbol s_1 is decoded correctly) are, respectively,

$$\gamma_{sr,SC}^{(1)} = \frac{\delta_{sr} \alpha_1 P_s(h_{sp})}{\delta_{sr} \alpha_2 P_s(h_{sp}) + 1}, \quad \gamma_{sr,SC}^{(2)} = \delta_{sr} \alpha_2 P_s(h_{sp}),$$

where $i^* \triangleq \operatorname{argmax}_{1 \leq i \leq N_r} |h_{sr,i}|$ and $\delta_{sr} \triangleq |h_{sr,i^*}|^2$. Similarly, the received instantaneous SINR at the SU-Rx for decoding symbol s_1 in the first time slot is given by

$$\gamma_{sd,SC} = \frac{\delta_{sd} \alpha_1 P_s(h_{sp})}{\delta_{sd} \alpha_2 P_s(h_{sp}) + 1},$$

where $j^* \triangleq \operatorname{argmax}_{1 \leq j \leq N_d} |h_{sd,j}|$ and $\delta_{sd} \triangleq |h_{sd,j^*}|^2$. The received SNR at the SU-Rx for decoding symbol s_2 in the second time slot is given by

$$\gamma_{rd,SC} = \delta_{rd} P_r(h_{rp}),$$

where $k^* \triangleq \operatorname{argmax}_{1 \leq k \leq N_d} |h_{rd,k}|$ and $\delta_{rd} \triangleq |h_{rd,k^*}|^2$. Following similar arguments as in the previous section, the average achievable rate for symbol s_1 using SC is given by

$$\bar{C}_{s_1,SC} = 0.5 \int_0^\infty \log_2(1 + Qx) f_{\mathcal{X}}(x) dx - 0.5 \int_0^\infty \log_2(1 + Q\alpha_2 x) f_{\mathcal{X}}(x) dx, \quad (15)$$

where $\mathcal{X} \triangleq \min\{\delta_{sr}, \delta_{sd}\} / \lambda_{sp}$.

Theorem 3. A closed-form expression for the average achievable rate for symbol s_1 using SC is given by

$$\bar{C}_{s_1,SC} = 0.5 \sum_{k=1}^{N_r} \sum_{j=1}^{N_d} (-1)^{k+j} \binom{N_r}{k} \binom{N_d}{j} \left[\frac{Q \log_2 \left(\frac{Q}{\xi_{k,j} \Omega_{sp}} \right)}{Q - \xi_{k,j} \Omega_{sp}} - \frac{\alpha_2 Q \log_2 \left(\frac{\alpha_2 Q}{\xi_{k,j} \Omega_{sp}} \right)}{\alpha_2 Q - \xi_{k,j} \Omega_{sp}} \right], \quad (16)$$

where $\xi_{k,j} \triangleq (k/\Omega_{sr}) + (j/\Omega_{sd})$.

Proof: See Appendix C.

Similarly, the average achievable rate for symbol s_2 using SC is given by

$$\bar{C}_{s_2,SC} = 0.5 \int_0^\infty \log_2(1 + Qx) f_{\mathcal{Y}}(x) dx, \quad (17)$$

where $\mathcal{Y} \triangleq \min\{\delta_{sr}a_2/\lambda_{sp}, \delta_{rd}/\lambda_{rp}\}$.

Theorem 4. *A closed-form expression for the average achievable rate for symbol s_2 using SC is given by*

$$\begin{aligned} \bar{C}_{s_2,SC} = 0.5Q & \left[\sum_{k=1}^{N_r} (-1)^{k-1} \binom{N_r}{k} \frac{a_2\Omega_{sr} \log_2\left(\frac{a_2\Omega_{sr}Q}{k\Omega_{sp}}\right)}{a_2\Omega_{sr}Q - k\Omega_{sp}} + \sum_{j=1}^{N_d} (-1)^{j-1} \binom{N_d}{j} \frac{\Omega_{rd} \log_2\left(\frac{\Omega_{rd}Q}{j\Omega_{rp}}\right)}{\Omega_{rd}Q - j\Omega_{rp}} \right. \\ & + \sum_{k=1}^{N_r} \sum_{j=1}^{N_d} (-1)^{k+j} \binom{N_r}{k} \binom{N_d}{j} \left\{ \frac{k\Omega_{rd}^2\Omega_{sp} \log_2\left(\frac{j\Omega_{rp}}{Q\Omega_{rd}}\right)}{(k\Omega_{rd}\Omega_{sp} - ja_2\Omega_{rp}\Omega_{sr})(Q\Omega_{rd} - j\Omega_{rp})} \right. \\ & \left. \left. + \frac{ja_2^2\Omega_{rp}\Omega_{sr}^2 \log_2\left(\frac{a_2Q\Omega_{sr}}{k\Omega_{sp}}\right)}{(k\Omega_{rd}\Omega_{sp} - ja_2\Omega_{rp}\Omega_{sr})(a_2Q\Omega_{sr} - k\Omega_{sp})} \right\} \right]. \quad (18) \end{aligned}$$

Proof: See Appendix D.

Using (16) and (18), the average achievable sum-rate for the CRS-NOMA system using SC is given by

$$\bar{C}_{sum,SC} = \bar{C}_{s_1,SC} + \bar{C}_{s_2,SC}. \quad (19)$$

With extensive algebraic manipulations, it can be shown that for $N_r = N_d = 1$, (16) and (18) reduces to (4) and (9), respectively. For the case of SS-based CRS-OMA with SC, the average achievable rate is given as

$$\bar{C}_{OMA,SC} = 0.5E_{\mathcal{Z}} [\log_2(1 + Q\mathcal{Z})], \quad (20)$$

where $\mathcal{Z} \triangleq \min\{\frac{\delta_{sr}}{\lambda_{sp}}, \frac{\delta_{sd}}{\lambda_{sp}} + \frac{\delta_{rd}}{\lambda_{rp}}\}$.

Outage probability for CRS-NOMA with SC: Similar to the previous section, we define Θ_1 as the outage event for symbol s_1 . Hence the outage probability for symbol s_1 using SC is given by

$$\begin{aligned} \Pr(\Theta_1) &= \Pr(C_{s_1,SC} < R_1) = \Pr(\mathcal{X} < \Theta_1) = \int_0^{\Theta_1} f_{\mathcal{X}}(x) dx \\ &= \sum_{k=1}^{N_r} \sum_{j=1}^{N_d} (-1)^{k+j} \binom{N_d}{j} \binom{N_r}{k} \frac{\xi_{k,j}\Omega_{sp}\Theta_1}{1 + \xi_{k,j}\Omega_{sp}\Theta_1}, \quad (21) \end{aligned}$$

where $C_{s_1,SC}$ is the instantaneous achievable rate for symbol s_1 in the SS-based CRS-NOMA using SC. The integration above is solved using (40) and [20, Eqn. (3.194-1), p. 315]. Next, we define \mathcal{O}_2 as the outage event for symbol s_2 using SC, similar to the previous section. Hence, the outage probability for symbol s_2 is given by

$$\Pr(\mathcal{O}_2) = F_{\frac{\delta_{sr}}{\lambda_{sp}}}(\Theta) + F_{\frac{\delta_{rd}}{\lambda_{rp}}}\left(\frac{\epsilon_2}{Q}\right) - F_{\frac{\delta_{sr}}{\lambda_{sp}}}(\Theta)F_{\frac{\delta_{rd}}{\lambda_{rp}}}\left(\frac{\epsilon_2}{Q}\right). \quad (22)$$

Using (22) and (42), the closed-form expression for the outage probability of symbol s_2 in SS-based CRS-NOMA using SC is given by

$$\begin{aligned} \Pr(\mathcal{O}_2) = & \sum_{k=1}^{N_r} \binom{N_r}{k} \frac{(-1)^{k-1} k \Omega_{sp} \Theta}{\Omega_{sr} + k \Omega_{sp} \Theta} + \sum_{j=1}^{N_d} \binom{N_d}{j} \frac{(-1)^{j-1} j \epsilon_2 \Omega_{rp}}{Q \Omega_{rd} + j \epsilon_2 \Omega_{rp}} \\ & - \sum_{k=1}^{N_r} \sum_{j=1}^{N_d} \binom{N_r}{k} \binom{N_d}{j} \frac{(-1)^{k+j} k j \Omega_{sp} \Omega_{rp} \epsilon_2 \Theta}{(\Omega_{sr} + k \Omega_{sp} \Theta)(\Omega_{rd} Q + j \Omega_{rp} \epsilon_2)}. \quad (23) \end{aligned}$$

On the other hand, the outage probability for the SS-based CRS-OMA with SC is given by

$$\Pr(\mathcal{O}_{OMA}) = \Pr(\mathcal{Z} < \epsilon_1).$$

Asymptotic behavior of CRS-NOMA with SC

Using (21), for large values of Q ,

$$\Pr(\mathcal{O}_1) = \sum_{k=1}^{N_r} \sum_{j=1}^{N_d} \sum_{n=0}^{\infty} (-1)^{k+j+n} \binom{N_d}{j} \binom{N_r}{k} \xi_{k,j}^{n+1} \left[\frac{\Omega_{sp} \epsilon_1}{(\alpha_1 - \epsilon_1 \alpha_2) Q} \right]^{n+1}.$$

Using [20, Eqn. (0.154-3), p. 4], we have

$$\Pr(\mathcal{O}_1) = \sum_{k=1}^{N_r} \sum_{j=1}^{N_d} \sum_{n=\min\{N_r, N_d\}-1}^{\infty} (-1)^{k+j+n} \binom{N_d}{j} \binom{N_r}{k} \xi_{k,j}^{n+1} \left[\frac{\Omega_{sp} \epsilon_1}{(\alpha_1 - \epsilon_1 \alpha_2) Q} \right]^{n+1} \propto Q^{-\min\{N_r, N_d\}}.$$

Therefore, it is clear that for the case of SS-based CRS-NOMA, the outage probability for s_1 decays as $Q^{-\min\{N_r, N_d\}}$ for large Q values. Using a similar identity, it can be shown that $F_{\delta_{sr}/\lambda_{sp}}(\Theta)$ decays as Q^{-N_r} , $F_{\delta_{rd}/\lambda_{rp}}(\epsilon_2/Q)$ decays as Q^{-N_d} and $F_{\delta_{sr}/\lambda_{sp}}(\Theta)F_{\delta_{rd}/\lambda_{rp}}(\epsilon_2/Q)$ decays as $Q^{-(N_r+N_d)}$ for large values of Q . Therefore, using (22), it follows that for the case of SS-based CRS-NOMA, the outage probability for s_2 decays as $Q^{-\min\{N_r, N_d\}}$ for large values of Q .

V. Performance Analysis: Maximal Ratio Combining

In this section, we analyze the scenario when $N_r \geq 1$, $N_d \geq 1$ and MRC is used for combining the signals at the relay and the SU-Rx. The received instantaneous SINR at the relay for

decoding symbol s_1 and the instantaneous SNR for decoding symbol s_2 (assuming the symbol s_1 is decoded correctly) in the first time slot are, respectively,

$$\gamma_{sr,MRC}^{(1)} = \frac{\eta_{sr} a_1 P_s(h_{sp})}{\eta_{sr} a_2 P_s(h_{sp}) + 1}, \quad \gamma_{sr,MRC}^{(2)} = \eta_{sr} a_2 P_s(h_{sp}),$$

where $\eta_{sr} \triangleq \sum_{i=1}^{N_r} |h_{sr,i}|^2$. Similarly, the received instantaneous SINR at the SU-Rx for decoding symbol s_1 in the first time slot is given by

$$\gamma_{sd,MRC} = \frac{\eta_{sd} a_1 P_s(h_{sp})}{\eta_{sd} a_2 P_s(h_{sp}) + 1},$$

where $\eta_{sd} \triangleq \sum_{j=1}^{N_d} |h_{sd,j}|^2$. The received SNR at the SU-Rx for decoding symbol s_2 in the second time slot is given by

$$\gamma_{rd,MRC} = \eta_{rd} P_r(h_{rp}),$$

where $\eta_{rd} \triangleq \sum_{k=1}^{N_d} |h_{rd,k}|^2$. The average achievable rate for symbol s_1 using MRC is given by

$$\bar{C}_{s_1,MRC} = 0.5 \int_0^\infty \log_2(1 + Qx) f_X(x) dx - 0.5 \int_0^\infty \log_2(1 + Qa_2x) f_X(x) dx, \quad (24)$$

where $X \triangleq \min\{\eta_{sr}, \eta_{sd}\}/\lambda_{sp}$.

Theorem 5. A closed-form expression for the average achievable rate for symbol s_1 using MRC is given by

$$\begin{aligned} \bar{C}_{s_1,MRC} = & 0.5 \log_2(e) \left[\frac{1}{\Gamma(N_r) \Omega_{sr}^{N_r}} \sum_{\nu=0}^{N_d-1} \frac{\left\{ G_{3,3}^{2,3} \left(\frac{Q}{\phi \Omega_{sp}} \middle| \begin{matrix} 1-N_r-\nu, 1, 1 \\ 1, 1, 0 \end{matrix} \right) - G_{3,3}^{2,3} \left(\frac{a_2 Q}{\phi \Omega_{sp}} \middle| \begin{matrix} 1-N_r-\nu, 1, 1 \\ 1, 1, 0 \end{matrix} \right) \right\}}{\Gamma(\nu+1) \Omega_{sd}^\nu \phi^{N_r+\nu}} \right. \\ & \left. + \frac{1}{\Gamma(N_d) \Omega_{sd}^{N_d}} \sum_{\mu=0}^{N_r-1} \frac{\left\{ G_{3,3}^{2,3} \left(\frac{Q}{\phi \Omega_{sp}} \middle| \begin{matrix} 1-N_d-\mu, 1, 1 \\ 1, 1, 0 \end{matrix} \right) - G_{3,3}^{2,3} \left(\frac{a_2 Q}{\phi \Omega_{sp}} \middle| \begin{matrix} 1-N_d-\mu, 1, 1 \\ 1, 1, 0 \end{matrix} \right) \right\}}{\Gamma(\mu+1) \Omega_{sr}^\mu \phi^{N_d+\mu}} \right], \end{aligned} \quad (25)$$

where $\Gamma(\cdot)$ is the Gamma function and $G_{p,q}^{m,n}(\cdot | \cdot)$ is Meijer's G function.

Proof: See Appendix E.

Similarly, the average achievable rate for symbol s_2 using MRC is given by

$$\bar{C}_{s_2,MRC} = 0.5 \int_0^\infty \log_2(1 + Qx) f_Y(x) dx, \quad (26)$$

where $Y \triangleq \min\{\eta_{sr} a_2 / \lambda_{sp}, \eta_{rd} / \lambda_{rp}\}$.

Theorem 6. A closed-form expression for the average achievable rate for symbol s_2 using MRC is given by

$$\begin{aligned} \bar{C}_{s_2, \text{MRC}} = & \frac{0.5 \log_2(e) N_r}{\Gamma(N_r + 1)} G_{3,3}^{2,3} \left(\frac{a_2 \Omega_{sr} Q}{\Omega_{sp}} \middle| \begin{matrix} 1-N_r, 1, 1 \\ 1, 1, 0 \end{matrix} \right) + \frac{0.5 \log_2(e) N_d}{\Gamma(N_d + 1)} G_{3,3}^{2,3} \left(\frac{\Omega_{rd} Q}{\Omega_{rp}} \middle| \begin{matrix} 1-N_d, 1, 1 \\ 1, 1, 0 \end{matrix} \right) \\ & - \frac{0.5 \log_2(e)}{\Gamma(N_r) \Gamma(N_d)} \left(\frac{a_2 \Omega_{rp} \Omega_{sr}}{\Omega_{rd} \Omega_{sp}} \right)^{N_d} G_{1,1:2,2:2,2}^{1,1:1,2:1,2} \left(\begin{matrix} 1-N_r-N_d \\ 1-N_d \end{matrix} \middle| \begin{matrix} 1, 1 \\ 1, 0 \end{matrix} \middle| \begin{matrix} -N_d, 1-N_d \\ 0, -N_d \end{matrix} \middle| \frac{Q a_2 \Omega_{sr}}{\Omega_{sp}}, \frac{a_2 \Omega_{sr} \Omega_{rp}}{\Omega_{sp} \Omega_{rd}} \right) \\ & - \frac{0.5 \log_2(e)}{\Gamma(N_d) \Gamma(N_r)} \left(\frac{\Omega_{sp} \Omega_{rd}}{a_2 \Omega_{sr} \Omega_{rp}} \right)^{N_r} G_{1,1:2,2:2,2}^{1,1:1,2:1,2} \left(\begin{matrix} 1-N_r-N_d \\ 1-N_r \end{matrix} \middle| \begin{matrix} 1, 1 \\ 1, 0 \end{matrix} \middle| \begin{matrix} -N_r, 1-N_r \\ 0, -N_r \end{matrix} \middle| \frac{Q \Omega_{rd}}{\Omega_{rp}}, \frac{\Omega_{rd} \Omega_{sp}}{a_2 \Omega_{sr} \Omega_{rp}} \right), \end{aligned} \quad (27)$$

where $G_{p_1, q_1; p_2, q_2; p_3, q_3}^{m_1, n_1; m_2, n_2; m_3, n_3}(\cdot | \cdot | \cdot | \cdot, \cdot)$ denotes the EGBMGF² [25].

Proof: See Appendix F.

Using (25) and (27), the average achievable sum-rate for the SS-based CRS-NOMA using MRC is given by

$$\bar{C}_{\text{sum, MRC}} = \bar{C}_{s_1, \text{MRC}} + \bar{C}_{s_2, \text{MRC}}. \quad (28)$$

For the case of CRS-OMA with MRC, the average achievable rate is given as

$$\bar{C}_{\text{OMA-MRC}} = 0.5 E_{\mathcal{Z}} [\log_2(1 + Q\mathcal{Z})], \quad (29)$$

where $\mathcal{Z} \triangleq \min \left\{ \frac{\eta_{sr}}{\lambda_{sp}}, \frac{\eta_{sd}}{\lambda_{sp}} + \frac{\eta_{rd}}{\lambda_{rp}} \right\}$.

Outage probability for CRS-NOMA with MRC:

Similar to the previous cases, we define \mathcal{O}_1 as the outage event for symbol s_1 in SS-based CRS-NOMA using MRC. Hence the outage probability for symbol s_1 is given by

$$\Pr(\mathcal{O}_1) = \Pr(C_{s_1, \text{MRC}} < R_1) = \Pr(\mathcal{X} < \Theta_1) = \int_0^{\Theta_1} f_{\mathcal{X}}(x) dx.$$

²Efficient Mathematica[®] implementations of EGBMGF are given in [22, Table II] and [23]; and a Matlab[®] implementation is given in [24].

Substituting the expression for $f_X(x)$ from (51) into the equation above and solving the integral using [20, Eqn. (3.194-1), p. 315], the outage probability for symbol s_1 in CRS-NOMA using MRC is given by

$$\begin{aligned} \Pr(\mathcal{O}_1) &= \underbrace{\frac{1}{\Gamma(N_r)\Omega_{sr}^{N_r}} \sum_{\nu=0}^{N_d-1} (\nu+1)_{N_r} \frac{(\Omega_{sp}\Theta_1)^{N_r+\nu}}{\Omega_{sd}^\nu(N_r+\nu)} {}_2F_1(N_r+\nu+1, N_r+\nu; N_r+\nu+1; -\Omega_{sp}\phi\Theta_1)}_{\mathcal{T}_1} \\ &+ \underbrace{\frac{1}{\Gamma(N_d)\Omega_{sd}^{N_d}} \sum_{\mu=0}^{N_r-1} (\mu+1)_{N_d} \frac{(\Omega_{sp}\Theta_1)^{N_d+\mu}}{\Omega_{sr}^\mu(N_d+\mu)} {}_2F_1(N_d+\mu+1, N_d+\mu; N_d+\mu+1; -\Omega_{sp}\phi\Theta_1)}_{\mathcal{T}_2}, \end{aligned} \quad (30)$$

where $(x)_n \triangleq \Gamma(x+n)/\Gamma(x)$ denotes the Pochhammer symbol. Next, we define \mathcal{O}_2 as the outage event for symbol s_2 using MRC, similar to the previous cases. Hence, the outage probability for symbol s_2 is given by

$$\Pr(\mathcal{O}_2) = F_{\frac{n_{sr}}{\lambda_{sp}}}(\Theta) + F_{\frac{n_{rd}}{\lambda_{rp}}} \left(\frac{\epsilon_2}{Q} \right) - F_{\frac{n_{sr}}{\lambda_{sp}}}(\Theta) F_{\frac{n_{rd}}{\lambda_{rp}}} \left(\frac{\epsilon_2}{Q} \right).$$

Using (54), the analytical expression for the outage probability of symbol s_2 for SS-based CRS-NOMA using MRC is represented by

$$\begin{aligned} \Pr(\mathcal{O}_2) &= \left(\frac{\Theta\Omega_{sp}}{\Omega_{sr}} \right)^{N_r} {}_2F_1 \left(N_r+1, N_r; N_r+1; \frac{-\Theta\Omega_{sp}}{\Omega_{sr}} \right) + \left(\frac{\epsilon_2\Omega_{rp}}{Q\Omega_{rd}} \right)^{N_d} {}_2F_1 \left(N_d+1, N_d; N_d+1; \frac{-\epsilon_2\Omega_{rp}}{Q\Omega_{rd}} \right) \\ &- \left(\frac{\Theta\Omega_{sp}}{\Omega_{sr}} \right)^{N_r} \left(\frac{\epsilon_2\Omega_{rp}}{Q\Omega_{rd}} \right)^{N_d} {}_2F_1 \left(N_r+1, N_r; N_r+1; \frac{-\Theta\Omega_{sp}}{\Omega_{sr}} \right) {}_2F_1 \left(N_d+1, N_d; N_d+1; \frac{-\epsilon_2\Omega_{rp}}{Q\Omega_{rd}} \right). \end{aligned} \quad (31)$$

On the other hand, the outage probability for the SS-based CRS-OMA with MRC is given by

$$\Pr(\mathcal{O}_{OMA}) = \Pr(\mathcal{Z} < \epsilon_1).$$

Asymptotic behavior of CRS-NOMA with MRC

Using the series expansion of the Gauss hypergeometric function [26, Eqn. (15.2.1). p. 384],

$$\begin{aligned} \mathcal{T}_1 &= \frac{1}{\Gamma(N_r)\Omega_{sr}^{N_r}} \sum_{\nu=0}^{N_d-1} \sum_{n=0}^{\infty} \frac{(\nu+1)_{N_r} \Omega_{sp}^{N_r+\nu} \epsilon_1^{N_r+\nu}}{\Omega_{sd}^\nu(N_r+\nu)(a_1 - \epsilon_1 a_2)^{N_r+\nu} Q^{N_r+\nu}} \frac{(-1)^n (N_r+\nu)_n (\Omega_{sp}\phi\epsilon_1)^n}{n! (a_1 - \epsilon_1 a_2)^n Q^n} \\ &= \left[\frac{\Omega_{sp}\epsilon_1}{\Omega_{sr}(a_1 - \epsilon_1 a_2)Q} \right]^{N_r} + \mathbf{o} \left(Q^{-(N_r+1)} \right). \end{aligned}$$

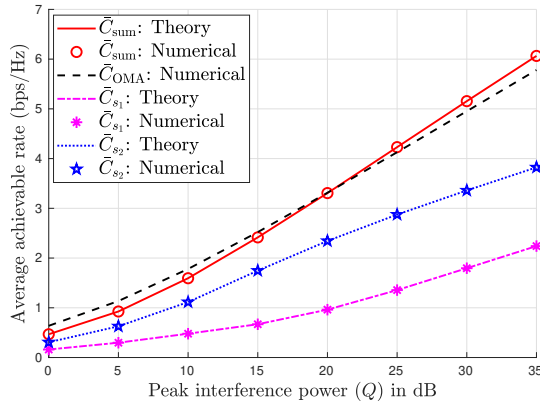


Fig. 2: Comparison of the average achievable rate for the SS-based CRS with $N_r = N_d = 1$.

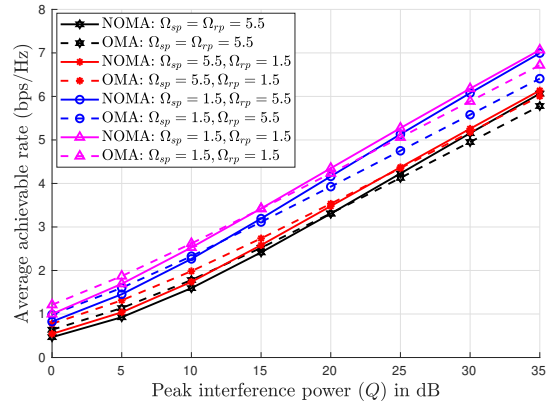


Fig. 3: Effect of the interference channels on the average achievable rate for the SS-based CRS.

Therefore, it is clear that \mathcal{T}_1 decays as Q^{-N_r} for large values of Q . Using similar arguments, it can be shown that \mathcal{T}_2 in (30) decays as Q^{-N_d} for large values of Q . Hence, it is straightforward to conclude that the outage probability for s_1 in CRS-NOMA with MRC decays as $Q^{-\min\{N_r, N_d\}}$ for large values of Q . Similarly, using the series expansion of the Gauss hypergeometric functions in (31), it can be shown that the outage probability for s_2 in CRS-NOMA with MRC decays as $Q^{-\min\{N_r, N_d\}}$ for large values of Q .

VI. Results and Discussion

In this section, we present the analytical and numerical³ results for the average achievable rate and outage probability for the spectrum sharing based cooperative relaying system. We consider the SS-based CRS system where $\Omega_{sd} = 1$, $\Omega_{sr} = \Omega_{rd} = 10$ and $\Omega_{sp} = \Omega_{rp} = 5.5$ (unless otherwise stated). For all NOMA based systems, we consider $R_1 = R_2 = 1$ bps/Hz.

The necessary constraint $a_1 > \epsilon_1 a_2$ (as noted in Section III) implies a possible range $0 < a_2 < 2^{-2R_1}$. Therefore the optimization of a_2 was performed using a one-dimensional search over the M -element discrete set $a_2 \in \{\epsilon, 2\epsilon, 3\epsilon, \dots, M\epsilon\}$, where M is a positive integer and $\epsilon = 2^{-2R_1}/(M+1)$. In this paper, we consider $M = 24$ ($\epsilon = 0.01$). All results for NOMA-based systems presented in this section will be for the optimized power allocation.

Fig. 2 shows a comparison of the average achievable rate for the SS-based CRS with $N_r = N_d = 1$. It is clear from the figure that for small values of peak interference power constraint Q ,

³For our numerical results, we do not realize the actual scenario, but rather generate the random variables and then evaluate the average achievable rate.

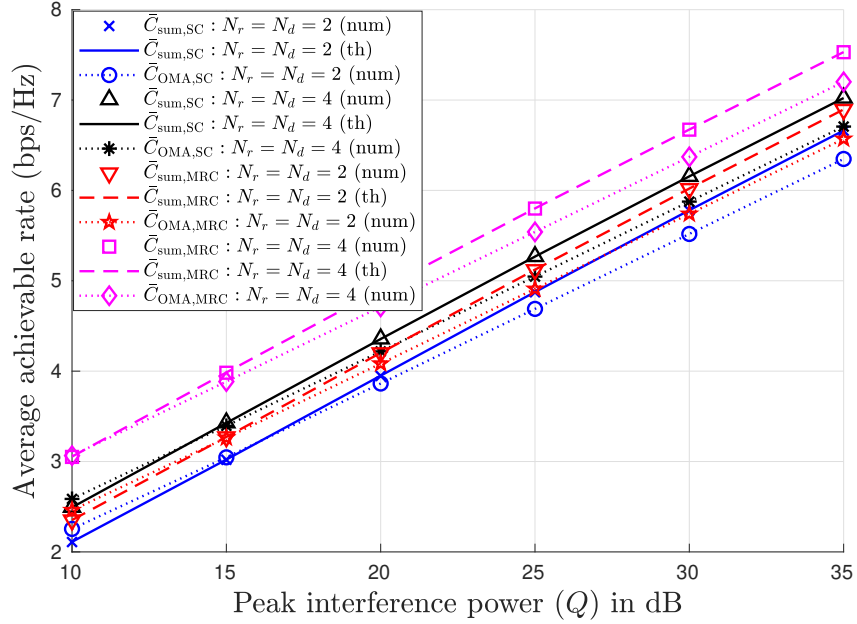


Fig. 4: Comparison of average achievable rate for SS-based CRS using SC and MRC for $\Omega_{sp} = \Omega_{sp} = 5.5$.

the SS-based CRS-OMA gives higher achievable rate, but for large values of Q , the SS-based CRS-NOMA outperforms its OMA-based counterpart and achieves higher spectral efficiency. This is due to the fact that for small values of Q , the average transmit power from the SU-Tx and the relay is small, and for small transmit SNR, the average achievable sum-rate of CRS-NOMA is less than the average achievable rate of CRS-OMA as shown in [10, Fig. 1].

Fig. 3 shows the effect of the mean-square value of the interference links (i.e., Ω_{sp} and Ω_{rp}) on the average achievable rate. The figures shows that when the interference links are weaker (in terms of mean-square value) the CRS achieves higher spectral efficiency. Moreover, it is clear from the figure that when the S-P link is weaker as compared to the R-P link (i.e., $\Omega_{sp} = 1.5$ and $\Omega_{rp} = 5.5$), the achievable rate of the CRS is comparatively higher than for the case when the former is stronger (i.e., $\Omega_{sp} = 5.5$ and $\Omega_{rp} = 1.5$). This means that the S-P interference channel has a more severe effect on the overall achievable rate of the CRS. This is due to the fact that when the interference channel between the SU-Tx and the PU-Rx is strong (i.e., Ω_{sp} is large), the average power transmitted from the SU-Tx is small which adversely effects the achievable rate of both s_1 and s_2 , while for the case when the interference channel between the relay and the PU-Rx is strong (i.e., Ω_{rp} is large) the average power transmitted from the relay

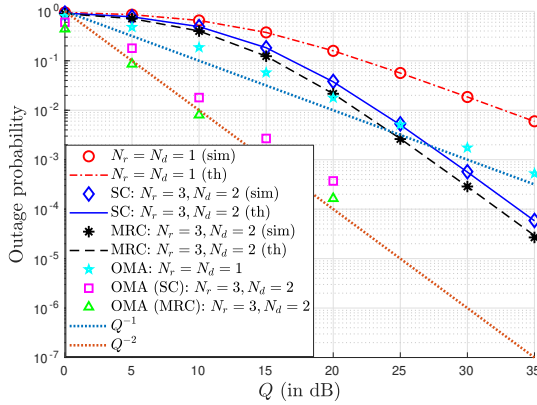


Fig. 5: Outage probability of symbol s_1 for the SS-based CRS.

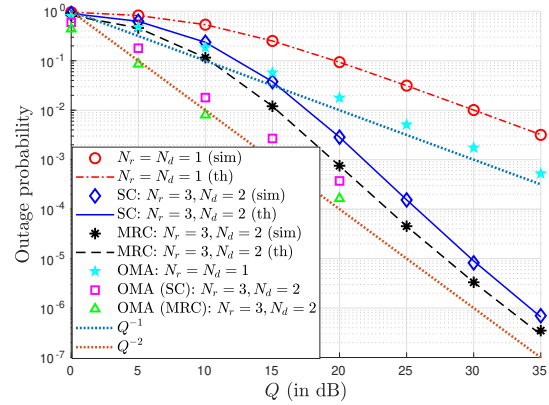


Fig. 6: Outage probability of symbol s_2 for the SS-based CRS.

is small which affects the achievable rate of symbol s_2 only.

Fig. 4 shows the average achievable rate for the SS-based CRS using selection combining and maximal-ratio combining for different values of N_r and N_d . It is evident from the figure that with an increase in the number of antennas at the relay and at the SU-Rx, the average achievable rate increases for both NOMA and OMA systems. Also, it is important to note that with this increase in the number of antennas, the threshold value of Q at which the CRS-NOMA outperforms its OMA-based counterpart becomes lower. Moreover, it is evident from the figure that CRS with MRC achieves significantly higher spectral efficiency as compared to that of CRS with SC for both NOMA and OMA systems.

Figs. 5 and 6 show the outage probabilities for SS-based CRS for s_1 and s_2 , respectively (in the case of SS-based CRS-OMA, both these figures show the outage probability of s_1 with a target data rate of 1 bps/Hz). It is evident from the figures that the outage probability for SS-based CRS-NOMA decreases significantly with an increase in the number of antennas at the relay and at the SU-Rx. Also, it can be noted from the figures that the outage probability of both the symbols with MRC is significantly lower than that with SC. These figures also confirm that for large values of Q , the outage probabilities decay as $Q^{-\min\{N_r, N_d\}}$, as proved analytically in the previous sections. The outage probability for the NOMA-based system is worse than that of the OMA-based system, because of the existence of co-channel interference and a higher

target data rate requirement in the case of CRS-NOMA⁴. Also it is important to note that the outage probability of symbol s_1 is higher than that of symbol s_2 for SS-based CRS-NOMA. This happens because the outage probability of s_1 is dominated by the links between SU-Tx and SU-Rx, which are the weakest (on average).

VII. Conclusion

In this paper, we provided a comprehensive average achievable sum-rate and outage probability analysis of a NOMA-based cooperative relaying system with underlay spectrum sharing considering a peak interference constraint in Rayleigh fading. We considered scenarios where the relay and the secondary receiver are equipped with multiple receive antennas and where both apply selection combining/maximal-ratio combining for signal reception. We also derived simplified analytical expressions for the special case when there is a single receive antenna at both relay and secondary-user receiver. Our results show that the optimal power allocation for maximizing the achievable sum-rate of CRS-NOMA depends on the target data rate requirement. It was shown that for higher values of peak interference power Q , the spectrum sharing system based on CRS-NOMA outperforms the spectrum sharing system based on conventional CRS-OMA, achieving higher spectral efficiency, for both SC and MRC schemes. Results also indicate that the interference channel between the secondary-user transmitter and the primary-user receiver has a more severe effect on the spectral efficiency of the secondary network as compared to that between the relay to the primary-user receiver interference channel. For a better insight into system behavior, we also presented the asymptotic (in the peak interference power) outage behavior for the SS-based CRS-NOMA. Our results also indicate that significant capacity gains can be achieved when the interference channel between the secondary-user transmitter/relay to primary-user receiver is in a deep fade.

Appendix A

Proof of Theorem 1

Since $|h_i|, i \in \{sr, sd, rd, sp, rp\}$ is Rayleigh distributed, the PDF and the CDF of $\lambda_i = |h_i|^2$ are, respectively, given by

$$f_{\lambda_i}(x) = \frac{1}{\Omega_i} \exp\left(\frac{-x}{\Omega_i}\right), F_{\lambda_i}(x) = 1 - \exp\left(\frac{-x}{\Omega_i}\right). \quad (32)$$

⁴Note that in the case of CRS-NOMA, *two symbols* were transmitted in the first time slot with target data rate of 1 bps/Hz for each, whereas in the case of CRS-OMA, only a *single symbol* was transmitted in the first time slot with a target data rate of 1 bps/Hz.

Therefore, the PDF of $\min\{\lambda_{sr}, \lambda_{sd}\}$ is given by⁵

$$f_{\min\{\lambda_{sr}, \lambda_{sd}\}}(x) = f_{\lambda_{sr}}(x)[1 - F_{\lambda_{sd}}(x)] + f_{\lambda_{sd}}(x)[1 - F_{\lambda_{sr}}(x)] = \phi \exp(-\phi x),$$

where $\phi = (1/\Omega_{sr}) + (1/\Omega_{sd})$. The PDF of $X = \min\{\lambda_{sr}, \lambda_{sd}\}/\lambda_{sp}$ is therefore given by

$$f_X(x) = \int_0^\infty y f_{\min\{\lambda_{sr}, \lambda_{sd}\}}(yx) f_{\lambda_{sp}}(y) dy = \frac{\phi}{\Omega_{sp}} \int_0^\infty y \exp\left[-\left(\phi x + \frac{1}{\Omega_{sp}}\right)y\right] dy = \frac{\phi \Omega_{sp}}{(1 + \phi \Omega_{sp} x)^2}. \quad (33)$$

The integral above is solved using [20, Eqn. (3.351-3), p. 340]. Using (33), the first integral in (3) can be solved as

$$I_1 \triangleq \log_2(e) \phi \Omega_{sp} \int_0^\infty \frac{\ln(1 + Qx) dx}{(1 + \phi \Omega_{sp} x)^2} = \frac{Q \log_2\left(\frac{Q}{\phi \Omega_{sp}}\right)}{Q - \phi \Omega_{sp}}. \quad (34)$$

The integration above is solved using [20, Eqn. (4.291-17)]. Similarly, the second integral in (3) can be solved by replacing Q in (34) with $a_2 Q$. Hence, using (3) and (34), the closed-form expression for the average achievable rate for symbol s_1 in SS-based CRS-NOMA system reduces to (4).

Appendix B

Proof of Theorem 2

Using (32) and a transformation of random variables, we have

$$f_{\lambda_{sr} a_2}(x) = \frac{1}{a_2} f_{\lambda_{sr}}\left(\frac{x}{a_2}\right) = \frac{1}{a_2 \Omega_{sr}} \exp\left(\frac{-x}{a_2 \Omega_{sr}}\right).$$

Hence,

$$\begin{aligned} f_{\lambda_{sr} a_2 / \lambda_{sp}}(x) &= \int_0^\infty y f_{\lambda_{sr} a_2}(yx) f_{\lambda_{sp}}(y) dy = \frac{1}{a_2 \Omega_{sr} \Omega_{sp}} \int_0^\infty y \exp\left[-\left(\frac{x}{a_2 \Omega_{sr}} + \frac{1}{\Omega_{sp}}\right)y\right] dy \\ &= \frac{a_2 \Omega_{sr} \Omega_{sp}}{(a_2 \Omega_{sr} + \Omega_{sp} x)^2}, \end{aligned} \quad (\text{using [20, 3.351-3, p. 340]})$$

and

$$F_{\lambda_{sr} a_2 / \lambda_{sp}}(x) = \int_0^x f_{\lambda_{sr} a_2 / \lambda_{sp}}(t) dt = \frac{\Omega_{sp} x}{a_2 \Omega_{sr} + \Omega_{sp} x}. \quad (35)$$

⁵Given two random variables \mathcal{U} and \mathcal{V} with PDFs $f_{\mathcal{U}}(x)$ and $f_{\mathcal{V}}(x)$ respectively, and CDFs $F_{\mathcal{U}}(x)$ and $F_{\mathcal{V}}(x)$ respectively, the PDF of $\mathcal{W} \triangleq \min\{\mathcal{U}, \mathcal{V}\}$ is given by $f_{\mathcal{W}}(x) = f_{\mathcal{U}}(x)[1 - F_{\mathcal{V}}(x)] + f_{\mathcal{V}}(x)[1 - F_{\mathcal{U}}(x)]$ and the CDF of \mathcal{W} is given by $F_{\mathcal{W}}(x) = F_{\mathcal{U}}(x) + F_{\mathcal{V}}(x) - F_{\mathcal{U}}(x)F_{\mathcal{V}}(x)$.

The integration above is solved using [20, Eqn. (3.194-1)]. Similarly, the CDF of $\lambda_{rd}/\lambda_{rp}$ can be expressed by replacing $a_2\Omega_{sr}$ and Ω_{sp} in (35) with Ω_{rd} and Ω_{rp} , respectively. Therefore, we have

$$1 - F_Y(x) = 1 - F_{\frac{\lambda_{sr}a_2}{\lambda_{sp}}}(x) - F_{\frac{\lambda_{rd}}{\lambda_{rp}}}(x) + F_{\frac{\lambda_{rd}}{\lambda_{rp}}}(x)F_{\frac{\lambda_{sr}a_2}{\lambda_{sp}}}(x) = \frac{a_2\Omega_{sr}\Omega_{rd}}{(a_2\Omega_{sr} + \Omega_{sp}x)(\Omega_{rd} + \Omega_{rp}x)}. \quad (36)$$

Using (8) and (36), the average achievable rate for symbol s_2 is given as

$$\bar{C}_{s_2} = \lim_{\Lambda \rightarrow \infty} \int_0^\Lambda \frac{0.5 \log_2(e) Q a_2 \Omega_{sr} \Omega_{rd} dx}{(a_2\Omega_{sr} + \Omega_{sp}x)(\Omega_{rd} + \Omega_{rp}x)(1 + Qx)}. \quad (37)$$

Solving the integral above using partial fractions, (37) reduces to (9); this completes the proof.

Appendix C

Proof of Theorem 3

The CDF and PDF of δ_{sr} (maximum of exponentially-distributed independent random variables) are, respectively,

$$F_{\delta_{sr}}(x) = 1 - \sum_{k=1}^{N_r} (-1)^{k-1} \binom{N_r}{k} \exp\left(\frac{-kx}{\Omega_{sr}}\right), \quad (38)$$

$$f_{\delta_{sr}}(x) = \sum_{k=1}^{N_r} (-1)^{k-1} \binom{N_r}{k} \frac{k}{\Omega_{sr}} \exp\left(\frac{-kx}{\Omega_{sr}}\right). \quad (39)$$

The CDF and PDF of δ_{sd} can be represented by replacing N_r and Ω_{sr} , respectively, by N_d and Ω_{sd} , respectively, in both (38) and (39). The PDF of $\min\{\delta_{sr}, \delta_{sd}\}$ is given by

$$f_{\min\{\delta_{sr}, \delta_{sd}\}}(x) = \sum_{k=1}^{N_r} \sum_{j=1}^{N_d} (-1)^{k+j} \binom{N_r}{k} \binom{N_d}{j} \xi_{k,j} \exp(-\xi_{k,j}x),$$

where $\xi_{k,j} = (k/\Omega_{sr}) + (j/\Omega_{sd})$. The PDF of $\mathcal{X} = \frac{\min\{\delta_{sr}, \delta_{sd}\}}{\lambda_{sp}}$ is therefore given by

$$\begin{aligned} f_{\mathcal{X}}(x) &= \int_0^\infty y f_{\min\{\delta_{sr}, \delta_{sd}\}}(yx) f_{\lambda_{sp}}(y) dy \\ &= \sum_{k=1}^{N_r} \sum_{j=1}^{N_d} \binom{N_r}{k} \binom{N_d}{j} \frac{(-1)^{k+j} \xi_{k,j}}{\Omega_{sp}} \int_0^\infty y \exp\left[-\left(\xi_{k,j}x + \frac{1}{\Omega_{sp}}\right)y\right] dy \\ &= \sum_{k=1}^{N_r} \sum_{j=1}^{N_d} \binom{N_r}{k} \binom{N_d}{j} \frac{(-1)^{k+j} \xi_{k,j}}{\Omega_{sp}} \left(\xi_{k,j}x + \frac{1}{\Omega_{sp}}\right)^{-2}. \end{aligned} \quad (40)$$

The integral above is solved using [20, Eqn. (3.351-3), p. 340]. Now, the first integral in (15) can be solved as

$$\begin{aligned}
I_2 &\triangleq \log_2(e) \int_0^\infty \ln(1+Qx) f_{\mathcal{X}}(x) dx \\
&= \sum_{k=1}^{N_r} \sum_{j=1}^{N_d} \binom{N_r}{k} \binom{N_d}{j} \frac{(-1)^{k+j} \xi_{k,j}}{\ln(2)\Omega_{sp}} \int_0^\infty \ln(1+Qx) \left(\xi_{k,j}x + \frac{1}{\Omega_{sp}} \right)^{-2} dx \\
&= \sum_{k=1}^{N_r} \sum_{j=1}^{N_d} \binom{N_r}{k} \binom{N_d}{j} \frac{(-1)^{k+j} Q}{Q - \xi_{k,j}\Omega_{sp}} \log_2 \left(\frac{Q}{\xi_{k,j}\Omega_{sp}} \right). \tag{41}
\end{aligned}$$

The integration above is solved using [20, Eqn. (4.291-17), p. 556]. Similarly, the second integral in (15) can be solved by replacing Q in (41) by a_2Q . Using (15) and (41), the closed-form expression for the average achievable rate for symbol s_1 in the CRS-NOMA system with SC reduces to (16); this completes the proof.

Appendix D

Proof of Theorem 4

Using (39) and a transformation of random variables, the PDF of $\delta_{sr}a_2$ is given by

$$f_{\delta_{sr}a_2}(x) = \frac{f_{\delta_{sr}}\left(\frac{x}{a_2}\right)}{a_2} = \sum_{k=1}^{N_r} \binom{N_r}{k} \frac{(-1)^{k-1}k}{a_2\Omega_{sr}} \exp\left(\frac{-kx}{a_2\Omega_{sr}}\right).$$

The PDF of $\delta_{sr}a_2/\lambda_{sp}$ is given by

$$\begin{aligned}
f_{\delta_{sr}a_2/\lambda_{sp}}(x) &= \int_0^\infty y f_{\delta_{sr}a_2}(yx) f_{\lambda_{sp}}(y) dy \\
&= \sum_{k=1}^{N_r} \binom{N_r}{k} \frac{(-1)^{k-1}k}{a_2\Omega_{sr}\Omega_{sp}} \int_0^\infty y \exp\left[-\left(\frac{kx}{a_2\Omega_{sr}} + \frac{1}{\Omega_{sp}}\right)y\right] dy = \sum_{k=1}^{N_r} \binom{N_r}{k} \frac{(-1)^{k-1}k}{a_2\Omega_{sr}\Omega_{sp}} \left(\frac{kx}{a_2\Omega_{sr}} + \frac{1}{\Omega_{sp}}\right)^{-2}.
\end{aligned}$$

The integration above is solved using [20, Eqn. (3.351-3), p. 340]. Using [20, Eqn. (3.194-1), p. 315], the CDF of $\delta_{sr}a_2/\lambda_{sp}$ is given by

$$F_{\frac{\delta_{sr}a_2}{\lambda_{sp}}}(x) = \int_0^x f_{\frac{\delta_{sr}a_2}{\lambda_{sp}}}(t) dt = \sum_{k=1}^{N_r} \binom{N_r}{k} \frac{(-1)^{k-1}k\Omega_{sp}x}{a_2\Omega_{sr} + k\Omega_{sp}x}. \tag{42}$$

Similarly, the CDF of δ_{rd}/δ_{rp} can be expressed by replacing N_r , $a_2\Omega_{sr}$ and Ω_{sp} in (42) by N_d , Ω_{rd} and Ω_{rp} , respectively. Therefore, for $\mathcal{Y} = \min\left\{\frac{\delta_{sr}a_2}{\lambda_{sp}}, \frac{\delta_{rd}}{\lambda_{rp}}\right\}$, we have

$$\begin{aligned}
1 - F_{\mathcal{Y}}(x) &= 1 - F_{\frac{\delta_{sr}a_2}{\lambda_{sp}}}(x) - F_{\frac{\delta_{rd}}{\lambda_{rp}}} + F_{\frac{\delta_{sr}a_2}{\lambda_{sp}}}(x) F_{\frac{\delta_{rd}}{\lambda_{rp}}}(x) = 1 - \sum_{k=1}^{N_r} \binom{N_r}{k} \frac{(-1)^{k-1}k\Omega_{sp}x}{a_2\Omega_{sr} + k\Omega_{sp}x} \\
&\quad - \sum_{j=1}^{N_d} \binom{N_d}{j} \frac{(-1)^{j-1}j\Omega_{rp}x}{\Omega_{rd} + j\Omega_{rp}x} + \sum_{k=1}^{N_r} \sum_{j=1}^{N_d} \binom{N_r}{k} \binom{N_d}{j} \frac{(-1)^{k+j}kj\Omega_{sp}\Omega_{rp}x^2}{(a_2\Omega_{sr} + k\Omega_{sp}x)(\Omega_{rd} + j\Omega_{rp}x)}. \tag{43}
\end{aligned}$$

Using (17), the average achievable rate for symbol s_2 using SC is given by

$$\bar{C}_{s_2,SC} = \frac{1}{2} \int_0^\infty \log_2(1 + Qx) f_Y(x) dx = \frac{0.5Q}{\ln(2)} \int_0^\infty \frac{1 - F_Y(x)}{1 + Qx} dx. \quad (44)$$

Now we define the integral I_3 as

$$\begin{aligned} I_3 &\triangleq \int_0^\infty \frac{1}{1 + Qx} \left(\frac{k\Omega_{sp}x}{a_2\Omega_{sr} + k\Omega_{sp}x} \right) dx = \int_0^\infty \frac{1}{1 + Qx} \left(1 - \frac{a_2\Omega_{sr}}{a_2\Omega_{sr} + k\Omega_{sp}x} \right) dx \\ &= \int_0^\infty \frac{1}{1 + Qx} dx - \lim_{\lambda \rightarrow \infty} \int_0^\lambda \frac{a_2\Omega_{sr} dx}{(a_2\Omega_{sr} + k\Omega_{sp}x)(1 + Qx)} = \int_0^\infty \frac{1}{1 + Qx} dx - \frac{a_2\Omega_{sr} \ln\left(\frac{a_2\Omega_{sr}Q}{k\Omega_{sp}}\right)}{a_2\Omega_{sr}Q - k\Omega_{sp}}. \end{aligned} \quad (45)$$

The integration above is solved using partial fractions. Similarly,

$$I_4 \triangleq \int_0^\infty \frac{1}{1 + Qx} \left(\frac{j\Omega_{rp}x}{\Omega_{rd} + j\Omega_{rp}x} \right) dx = \int_0^\infty \frac{1}{1 + Qx} dx - \frac{\Omega_{rd}}{\Omega_{rd}Q - j\Omega_{rp}} \ln\left(\frac{\Omega_{rd}Q}{j\Omega_{rp}}\right), \quad (46)$$

and

$$\begin{aligned} I_5 &\triangleq \int_0^\infty \frac{1}{1 + Qx} \left(\frac{kj\Omega_{sp}\Omega_{rp}x^2}{(a_2\Omega_{sr} + k\Omega_{sp}x)(\Omega_{rd} + j\Omega_{rp}x)} \right) dx \\ &= \int_0^\infty \frac{1}{1 + Qx} \left[1 + \frac{k\Omega_{rd}^2\Omega_{sp}}{(a_2j\Omega_{rp}\Omega_{sr} - k\Omega_{rd}\Omega_{sp})(\Omega_{rd} + j\Omega_{rp}x)} + \frac{a_2^2j\Omega_{rp}\Omega_{sr}^2}{(k\Omega_{rd}\Omega_{sp} - a_2j\Omega_{rp}\Omega_{sr})(a_2\Omega_{sr} + k\Omega_{sp}x)} \right] dx \\ &= \int_0^\infty \frac{1}{1 + Qx} dx + \frac{k\Omega_{rd}^2\Omega_{sp} \ln\left(\frac{j\Omega_{rp}}{\Omega_{rd}Q}\right)}{(k\Omega_{rd}\Omega_{sp} - a_2j\Omega_{rp}\Omega_{sr})(\Omega_{rd}Q - j\Omega_{rp})} + \frac{a_2^2j\Omega_{rp}\Omega_{sr}^2 \ln\left(\frac{a_2\Omega_{sr}Q}{k\Omega_{sp}}\right)}{(k\Omega_{rd}\Omega_{sp} - a_2j\Omega_{rp}\Omega_{sr})(a_2\Omega_{sr}Q - k\Omega_{sp})}. \end{aligned} \quad (47)$$

Moreover, we also have

$$\left[1 - \sum_{k=1}^{N_r} (-1)^{k-1} \binom{N_r}{k} - \sum_{j=1}^{N_d} (-1)^{j-1} \binom{N_d}{j} + \sum_{k=1}^{N_r} \sum_{j=1}^{N-d} (-1)^{k+j} \binom{N_r}{k} \binom{N_d}{j} \right] \int_0^\infty \frac{dx}{1 + Qx} = 0. \quad (48)$$

Using (44) – (48), the closed-form expression for the average achievable rate of symbol s_2 using SC reduces to (18); this completes the proof.

Appendix E

Proof of Theorem 5

Since $|h_{sr,i}|, \forall i \in \{1, 2, \dots, N_r\}$ is a Rayleigh distributed random variable, η_{sr} will be Gamma distributed. Therefore,

$$f_{\eta_{sr}}(x) = \frac{x^{N_r-1}}{\Gamma(N_r)\Omega_{sr}^{N_r}} \exp\left(\frac{-x}{\Omega_{sr}}\right), \quad (49)$$

$$F_{\eta_{sr}}(x) = 1 - \exp\left(\frac{-x}{\Omega_{sr}}\right) \sum_{\mu=0}^{N_r-1} \frac{1}{\mu!} \left(\frac{x}{\Omega_{sr}}\right)^\mu. \quad (50)$$

Similarly, the expression for $f_{\eta_{sd}}(x)$ and $F_{\eta_{sd}}(x)$ can be represented by replacing N_r and Ω_{sr} , respectively, by N_d and Ω_{sd} , respectively in both (49) and (50). Therefore,

$$\begin{aligned} f_{\min\{\eta_{sr}, \eta_{sd}\}}(x) &= f_{\eta_{sr}}(x)[1 - F_{\eta_{sd}}(x)] + f_{\eta_{sd}}(x)[1 - F_{\eta_{sr}}(x)] \\ &= \frac{\exp(-\phi x)}{\Gamma(N_r)\Omega_{sr}^{N_r}} \sum_{\nu=0}^{N_d-1} \frac{x^{N_r+\nu-1}}{\nu!\Omega_{sd}^\nu} + \frac{\exp(-\phi x)}{\Gamma(N_d)\Omega_{sd}^{N_d}} \sum_{\mu=0}^{N_r-1} \frac{x^{N_d+\mu-1}}{\mu!\Omega_{sr}^\mu}. \end{aligned}$$

Using a transformation of random variables yields

$$\begin{aligned} f_X(x) &= \int_0^\infty y f_{\min\{\eta_{sr}, \eta_{sd}\}}(yx) f_{\lambda_{sp}}(y) dy = \sum_{\nu=0}^{N_d-1} \frac{x^{N_r+\nu-1}}{\Gamma(N_r)\Omega_{sr}^{N_r}\Omega_{sp}\nu!\Omega_{sd}^\nu} \int_0^\infty y^{N_r+\nu} \exp\left[-\left(\phi x + \frac{1}{\Omega_{sp}}\right)y\right] dy \\ &+ \sum_{\mu=0}^{N_r-1} \frac{x^{N_d+\mu-1}}{\Gamma(N_d)\Omega_{sd}^{N_d}\Omega_{sp}\mu!\Omega_{sr}^\mu} \int_0^\infty y^{N_d+\mu} \exp\left[-\left(\phi x + \frac{1}{\Omega_{sp}}\right)y\right] dy = \sum_{\nu=0}^{N_d-1} \frac{x^{N_r+\nu-1} \Gamma(N_r + \nu + 1)}{\Gamma(N_r)\Gamma(\nu + 1)\Omega_{sr}^{N_r}\Omega_{sd}^\nu\Omega_{sp}} \\ &\times \left(\phi x + \frac{1}{\Omega_{sp}}\right)^{-(N_r+\nu+1)} + \sum_{\mu=0}^{N_r-1} \frac{x^{N_d+\mu-1} \Gamma(N_d + \mu + 1)}{\Gamma(N_d)\Gamma(\mu + 1)\Omega_{sd}^{N_d}\Omega_{sr}^\mu\Omega_{sp}} \left(\phi x + \frac{1}{\Omega_{sp}}\right)^{-(N_d+\mu+1)}. \end{aligned} \quad (51)$$

The integration above is solved using [20, Eqn. (3.351-3), p 340]. Substituting the expression for $f_X(x)$ from (51) into (24), and using [27, Eqn. (11)], the first integral in (24) can be solved as

$$\begin{aligned} I_6 &\triangleq 0.5 \log_2(e) \int_0^\infty G_{2,2}^{1,2} \left(Qx \mid \begin{matrix} 1, 1 \\ 1, 0 \end{matrix} \right) f_X(x) dx \\ &= 0.5 \log_2(e) \left[\sum_{\nu=0}^{N_d-1} \frac{\Gamma(N_r + \nu + 1) \int_0^\infty x^{N_r+\nu-1} \left(x + \frac{1}{\Omega_{sp}\phi}\right)^{-(N_r+\nu+1)} G_{2,2}^{1,2} \left(Qx \mid \begin{matrix} 1, 1 \\ 1, 0 \end{matrix} \right) dx}{\Gamma(N_r)\Gamma(\nu + 1)\Omega_{sr}^{N_r}\Omega_{sd}^\nu\Omega_{sp}\phi^{N_r+\nu+1}} \right. \\ &\quad \left. + \sum_{\mu=0}^{N_r-1} \frac{\Gamma(N_d + \mu + 1) \int_0^\infty x^{N_d+\mu-1} \left(x + \frac{1}{\phi\Omega_{sp}}\right)^{-(N_d+\mu+1)} G_{2,2}^{1,2} \left(Qx \mid \begin{matrix} 1, 1 \\ 1, 0 \end{matrix} \right) dx}{\Gamma(N_d)\Gamma(\mu + 1)\Omega_{sd}^{N_d}\Omega_{sr}^\mu\Omega_{sp}\phi^{N_d+\mu+1}} \right] \\ &= 0.5 \log_2(e) \left[\sum_{\nu=0}^{N_d-1} \frac{G_{3,3}^{2,3} \left(\frac{Q}{\phi\Omega_{sp}} \mid \begin{matrix} 1-N_r-\nu, 1, 1 \\ 1, 1, 0 \end{matrix} \right)}{\Gamma(N_r)\Gamma(\nu + 1)\Omega_{sr}^{N_r}\Omega_{sd}^\nu\phi^{N_r+\nu}} + \sum_{\mu=0}^{N_r-1} \frac{G_{3,3}^{2,3} \left(\frac{Q}{\phi\Omega_{sp}} \mid \begin{matrix} 1-N_d-\mu, 1, 1 \\ 1, 1, 0 \end{matrix} \right)}{\Gamma(N_d)\Gamma(\mu + 1)\Omega_{sd}^{N_d}\Omega_{sr}^\mu\phi^{N_d+\mu}} \right]. \end{aligned} \quad (52)$$

The integration above is solved using [20, Eqn. (7.811-5), p. 852]. Similarly, the second integral in (24) can be solved by replacing Q in (52) with a_2Q . Therefore, using (24) and (52), the analytical expression for the average achievable rate of symbol s_1 in the SS-based CRS-NOMA using MRC reduces to (25).

Appendix F

Proof of Theorem 6

Using (49) and a transformation of random variables, we have

$$f_{\eta_{sr}a_2}(x) = \frac{1}{a_2} f_{\eta_{sr}}\left(\frac{x}{a_2}\right) = \frac{x^{N_r-1}}{\Gamma(N_r)\Omega_{sr}^{N_r}a_2^{N_r}} \exp\left(\frac{-x}{a_2\Omega_{sr}}\right).$$

Therefore,

$$\begin{aligned} f_{\eta_{sr}a_2/\lambda_{sp}}(x) &= \int_0^\infty y f_{\eta_{sr}a_2}(yx) f_{\lambda_{sp}}(y) dy \\ &= \frac{x^{N_r-1}}{\Gamma(N_r)\Omega_{sr}^{N_r}a_2^{N_r}\Omega_{sp}} \int_0^\infty y^{N_r} \exp\left[-\left(\frac{x}{a_2\Omega_{sr}} + \frac{1}{\Omega_{sp}}\right)y\right] dy = \frac{N_r\Omega_{sr}a_2\Omega_{sp}^{N_r}x^{N_r-1}}{(a_2\Omega_{sr} + \Omega_{sp}x)^{N_r+1}}. \end{aligned} \quad (53)$$

The integration above is solved using [20, Eqn. (3.351-3), p.340]. Using (53), we have

$$F_{\frac{\eta_{sr}a_2}{\lambda_{sp}}}(x) = N_r\Omega_{sr}a_2\Omega_{sp}^{N_r} \int_0^x \frac{t^{N_r-1} dt}{(a_2\Omega_{sr} + \Omega_{sp}t)^{N_r+1}} = \left(\frac{\Omega_{sp}x}{a_2\Omega_{sr}}\right)^{N_r} {}_2F_1\left(N_r+1, N_r; N_r+1; \frac{-\Omega_{sp}}{a_2\Omega_{sr}}x\right), \quad (54)$$

where ${}_2F_1(\cdot, \cdot; \cdot; \cdot)$ is the Gauss hypergeometric function and the integration above is solved using [20, Eqn. (3.194-1), p. 315]. The PDF of η_{rd}/λ_{rp} can be expressed by replacing $N_r, a_2\Omega_{sr}$ and Ω_{sp} , respectively, in (53) by N_d, Ω_{rd} and Ω_{rp} , respectively. The CDF of η_{rd}/λ_{rp} can be expressed in a similar fashion using (54). Therefore, the PDF of \mathcal{Y} can be obtained as

$$\begin{aligned} f_{\mathcal{Y}}(x) &= f_{\eta_{sr}a_2/\lambda_{sp}}(x)[1 - F_{\eta_{rd}/\lambda_{rp}}(x)] + f_{\eta_{rd}/\lambda_{rp}}(x)[1 - F_{\eta_{sr}a_2/\lambda_{sp}}(x)] = \frac{N_r\Omega_{sr}a_2\Omega_{sp}^{N_r}x^{N_r-1}}{(a_2\Omega_{sr} + \Omega_{sp}x)^{N_r+1}} \\ &+ \frac{N_d\Omega_{rd}\Omega_{sp}^{N_d}x^{N_d-1}}{(\Omega_{rd} + \Omega_{rp}x)^{N_d+1}} - \frac{N_r\Omega_{sr}a_2\Omega_{sp}^{N_r}\Omega_{rp}^{N_d}x^{N_r+N_d-1}}{\Omega_{rd}^{N_d}(a_2\Omega_{sr} + \Omega_{sp}x)^{N_r+1}} {}_2F_1\left(N_d+1, N_d; N_d+1; \frac{-\Omega_{rp}}{\Omega_{rd}}x\right) \\ &- \frac{N_d\Omega_{rd}\Omega_{rp}^{N_d}\Omega_{sp}^{N_r}x^{N_r+N_d-1}}{a_2^{N_r}\Omega_{sr}^{N_r}(\Omega_{rd} + \Omega_{rp}x)^{N_d+1}} {}_2F_1\left(N_r+1, N_r; N_r+1; \frac{-\Omega_{sp}}{a_2\Omega_{sr}}x\right). \end{aligned} \quad (55)$$

Using (26) and (55), we have

$$\bar{C}_{s_2, \text{MRC}} = 0.5 \log_2(e) [I_7 + I_8 - I_9 - I_{10}], \quad (56)$$

where

$$\begin{aligned} I_7 &\triangleq \int_0^\infty \ln(1+Qx) \frac{N_r\Omega_{sr}a_2\Omega_{sp}^{N_r}x^{N_r-1}}{(a_2\Omega_{sr} + \Omega_{sp}x)^{N_r+1}} dx \\ &= \frac{N_r\Omega_{sr}a_2}{\Omega_{sp}} \int_0^\infty G_{2,2}^{1,2}\left(Qx \left| \begin{matrix} 1, 1 \\ 1, 0 \end{matrix} \right.\right) x^{N_r-1} \left(x + \frac{a_2\Omega_{sr}}{\Omega_{sp}}\right)^{-(N_r+1)} dx = \frac{N_r}{\Gamma(N_r+1)} G_{3,3}^{2,3}\left(\frac{a_2\Omega_{sr}Q}{\Omega_{sp}} \left| \begin{matrix} 1-N_r, 1, 1 \\ 1, 1, 0 \end{matrix} \right.\right). \end{aligned} \quad (57)$$

The integration above is solved using [20, Eqn. (7.811-5), p. 852]. Similarly,

$$I_8 \triangleq \int_0^\infty \ln(1+Qx) \frac{N_d\Omega_{rd}\Omega_{sp}^{N_d}x^{N_d-1}}{(\Omega_{rd} + \Omega_{rp}x)^{N_d+1}} dx = \frac{N_d}{\Gamma(N_d+1)} G_{3,3}^{2,3}\left(\frac{\Omega_{rd}Q}{\Omega_{rp}} \left| \begin{matrix} 1-N_d, 1, 1 \\ 1, 1, 0 \end{matrix} \right.\right). \quad (58)$$

$$I_9 \triangleq \frac{N_r \Omega_{sr} a_2 \Omega_{sp}^{N_r} \Omega_{rp}^{N_d}}{\Omega_{rd}^{N_d}} \int_0^\infty \ln(1 + Qx) \frac{x^{N_r+N_d-1}}{(a_2 \Omega_{sr} + \Omega_{sp} x)^{N_r+1}} {}_2F_1 \left(N_d + 1, N_d; N_d + 1; \frac{-\Omega_{rp}}{\Omega_{rd}} x \right) dx.$$

Using [27, Eqns. (11), (17)] and [28], I_9 can be represented as

$$\begin{aligned} I_9 &= \frac{N_r \Omega_{sp}^{N_r} \Omega_{rp}^{N_d} \int_0^\infty x^{N_r+N_d-1} G_{2,2}^{1,2} \left(Qx \left| \begin{matrix} 1, 1 \\ 1, 0 \end{matrix} \right. \right) G_{1,1}^{1,1} \left(\frac{\Omega_{sp} x}{a_2 \Omega_{sr}} \left| \begin{matrix} -N_r \\ 0 \end{matrix} \right. \right) G_{2,2}^{1,2} \left(\frac{\Omega_{rp}}{\Omega_{rd}} x \left| \begin{matrix} -N_d, 1-N_d \\ 0, -N_d \end{matrix} \right. \right) dx}{\Omega_{rd}^{N_d} a_2^{N_r} \Omega_{sr}^{N_r} \Gamma(N_r + 1) \Gamma(N_d)} \\ &= \frac{1}{\Gamma(N_r) \Gamma(N_d)} \left(\frac{a_2 \Omega_{rp} \Omega_{sr}}{\Omega_{rd} \Omega_{sp}} \right)^{N_d} G_{1,1:2,2;2}^{1,1:1,2;1,2} \left(\begin{matrix} 1-N_r-N_d \\ 1-N_d \end{matrix} \left| \begin{matrix} 1, 1 \\ 1, 0 \end{matrix} \right. \begin{matrix} -N_d, 1-N_d \\ 0, -N_d \end{matrix} \left| \begin{matrix} Q a_2 \Omega_{sr} \\ \Omega_{sp} \end{matrix}, \begin{matrix} a_2 \Omega_{sr} \Omega_{rp} \\ \Omega_{sp} \Omega_{rd} \end{matrix} \right. \right). \end{aligned} \quad (59)$$

The integration above is solved using [23, Eqn. (9)]. Similarly,

$$\begin{aligned} I_{10} &= \frac{N_d \Omega_{rd} \Omega_{rp}^{N_d} \Omega_{sp}^{N_r}}{a_2^{N_r} \Omega_{sr}^{N_r}} \int_0^\infty \ln(1 + Qx) \frac{x^{N_r+N_d-1}}{(\Omega_{rd} + \Omega_{rp} x)^{N_d+1}} {}_2F_1 \left(N_r + 1, N_r; N_r + 1; \frac{-\Omega_{sp}}{a_2 \Omega_{sr}} x \right) dx \\ &= \frac{1}{\Gamma(N_d) \Gamma(N_r)} \left(\frac{\Omega_{sp} \Omega_{rd}}{a_2 \Omega_{sr} \Omega_{rp}} \right)^{N_r} G_{1,1:2,2;2}^{1,1:1,2;1,2} \left(\begin{matrix} 1-N_r-N_d \\ 1-N_r \end{matrix} \left| \begin{matrix} 1, 1 \\ 1, 0 \end{matrix} \right. \begin{matrix} -N_r, 1-N_r \\ 0, -N_r \end{matrix} \left| \begin{matrix} Q \Omega_{rd} \\ \Omega_{rp} \end{matrix}, \begin{matrix} \Omega_{rd} \Omega_{sp} \\ a_2 \Omega_{sr} \Omega_{rp} \end{matrix} \right. \right). \end{aligned} \quad (60)$$

Using (26) and (56)-(60), the analytical expression for the average achievable rate of symbol s_2 in the SS-based CRS-NOMA using MRC reduces to (27); this completes the proof.

References

- [1] Z. Ding, X. Lei, G. K. Karagiannidis, R. Schober, J. Yuan, and V. K. Bhargava, "A survey on non-orthogonal multiple access for 5G networks: Research challenges and future trends," *IEEE J. Sel. Areas Commun.*, vol. 35, no. 10, pp. 2181–2195, Oct 2017.
- [2] Y. Liu, Z. Qin, M. ElKashlan, Z. Ding, A. Nallanathan, and L. Hanzo, "Nonorthogonal multiple access for 5G and beyond," *Proc. of the IEEE*, vol. 105, no. 12, pp. 2347–2381, Dec 2017.
- [3] Z. Ding, Y. Liu, J. Choi, Q. Sun, M. ElKashlan, C.-L. I, and H. V. Poor, "Application of non-orthogonal multiple access in LTE and 5G networks," *IEEE Commun. Mag.*, vol. 55, no. 2, pp. 185–191, February 2017.
- [4] Y. Saito, Y. Kishiyama, A. Benjebbour, T. Nakamura, A. Li, and K. Higuchi, "Non-orthogonal multiple access (NOMA) for cellular future radio access," in *2013 IEEE 77th Veh. Technol. Conf. (VTC Spring)*, June 2013, pp. 1–5.
- [5] M. Vaezi, Z. Ding, and H. Poor, *Multiple Access Techniques for 5G Wireless Networks and Beyond*. Springer International Publishing, 2018.
- [6] D. Fang, Y. Huang, Z. Ding, G. Geraci, S. Shieh, and H. Claussen, "Lattice partition multiple access: A new method of downlink non-orthogonal multiuser transmissions," in *2016 IEEE Global Commun. Conf. (GLOBECOM)*, Dec 2016, pp. 1–6.
- [7] A. Goldsmith, S. A. Jafar, I. Maric, and S. Srinivasa, "Breaking spectrum gridlock with cognitive radios: An information theoretic perspective," *Proc. of the IEEE*, vol. 97, no. 5, pp. 894–914, May 2009.
- [8] J. Bater, H.-P. Tan, K. N. Brown, and L. Doyle, "Modelling interference temperature constraints for spectrum access in cognitive radio networks," in *2007 IEEE Int. Conf. Commun. (ICC)*, June 2007, pp. 6493–6498.

- [9] A. Ghasemi and E. S. Sousa, "Fundamental limits of spectrum-sharing in fading environments," *IEEE Trans. Wireless Commun.*, vol. 6, no. 2, pp. 649–658, Feb 2007.
- [10] J. B. Kim and I. H. Lee, "Capacity analysis of cooperative relaying systems using non-orthogonal multiple access," *IEEE Commun. Lett.*, vol. 19, no. 11, pp. 1949–1952, Nov 2015.
- [11] R. Jiao, L. Dai, J. Zhang, R. MacKenzie, and M. Hao, "On the performance of NOMA-based cooperative relaying systems over Rician fading channels," *IEEE Trans. Veh. Technol.*, vol. 66, no. 12, pp. 11409–11413, Dec 2017.
- [12] L. Lv, J. Chen, Q. Ni, Z. Ding, and H. Jiang, "Cognitive non-orthogonal multiple access with cooperative relaying: A new wireless frontier for 5G spectrum sharing," *IEEE Commun. Mag.*, vol. 56, no. 4, pp. 188–195, Apr 2018.
- [13] M. Mohammadi, X. Shi, B. K. Chalise, Z. Ding, H. A. Suraweera, C. Zhong, and J. S. Thompson, "Full-duplex non-orthogonal multiple access for next generation wireless systems," *IEEE Commun. Mag.*, vol. 57, no. 5, pp. 110–116, May 2019.
- [14] B. Chen, Y. Chen, Y. Chen, Y. Cao, N. Zhao, and Z. Ding, "A novel spectrum sharing scheme assisted by secondary NOMA relay," *IEEE Wireless Commun. Lett.*, vol. 7, no. 5, pp. 732–735, Oct 2018.
- [15] L. Lv, Q. Ni, Z. Ding, and J. Chen, "Application of non-orthogonal multiple access in cooperative spectrum-sharing networks over nakagami- m fading channels," *IEEE Trans. Veh. Technol.*, vol. 66, no. 6, pp. 5506–5511, June 2017.
- [16] Y. Liu, Z. Ding, M. Elkashlan, and J. Yuan, "Nonorthogonal multiple access in large-scale underlay cognitive radio networks," *IEEE Trans. Veh. Technol.*, vol. 65, no. 12, pp. 10152–10157, Dec 2016.
- [17] Y. Zhang, Q. Yang, T. Zheng, H. Wang, Y. Ju, and Y. Meng, "Energy efficiency optimization in cognitive radio inspired non-orthogonal multiple access," in *2016 IEEE 27th Annual International Symposium on Personal, Indoor, and Mobile Radio Communications (PIMRC)*, Sep. 2016, pp. 1–6.
- [18] S. Arzykulov, T. A. Tsiftsis, G. Nauryzbayev, M. Abdallah, and G. Yang, "Outage performance of underlay CR-NOMA networks with detect-and-forward relaying," in *2018 IEEE Global Commun. Conf. (GLOBECOM)*, Dec 2018, pp. 1–6.
- [19] S. Arzykulov, T. A. Tsiftsis, G. Nauryzbayev, and M. Abdallah, "Outage performance of cooperative underlay CR-NOMA with imperfect CSI," *IEEE Commun. Lett.*, vol. 23, no. 1, pp. 176–179, Jan 2019.
- [20] A. Jeffrey and D. Zwillinger, *Table of Integrals, Series, and Products*, 7th ed. Elsevier Science, 2007.
- [21] Z. Ding, H. Dai, and H. V. Poor, "Relay selection for cooperative NOMA," *IEEE Wireless Commun. Lett.*, vol. 5, no. 4, pp. 416–419, Aug 2016.
- [22] I. S. Ansari, S. Al-Ahmadi, F. Yilmaz, M. Alouini, and H. Yanikomeroglu, "A new formula for the BER of binary modulations with dual-branch selection over generalized-K composite fading channels," *IEEE Trans. Commun.*, vol. 59, no. 10, pp. 2654–2658, Oct 2011.
- [23] C. García-Corrales, F. J. Cañete, and J. F. Paris, "Capacity of $\kappa - \mu$ shadowed fading channels," *International Journal of Antennas and Propagation*, vol. 24, 2014.
- [24] H. Chergui, M. Benjillali, and S. Saoudi, "Performance analysis of project-and-forward relaying in mixed MIMO-pinhole and rayleigh dual-hop channel," *IEEE Commun. Lett.*, vol. 20, no. 3, pp. 610–613, March 2016.
- [25] B. L. Sharma and R. F. A. Abiodun, "Generating function for generalized function of two variables," *Proceedings of the American Mathematical Society*, vol. 46, no. 1, pp. 69–72, 1974.

- [26] F. Olver, D. Lozier, R. Boisvert, and C. Clark, *NIST Handbook of Mathematical Functions Hardback*. Cambridge University Press, 2010.
- [27] V. S. Adamchik and O. I. Marichev, "The algorithm for calculating integrals of hypergeometric type functions and its realization in REDUCE system," in *Proceedings of the International Symposium on Symbolic and Algebraic Computation*. New York, NY, USA: ACM, 1990, pp. 212–224.
- [28] I. S. Ansari, F. Yilmaz, and M. Alouini, "Impact of pointing errors on the performance of mixed RF/FSO dual-hop transmission systems," *IEEE Wireless Commun. Lett.*, vol. 2, no. 3, pp. 351–354, June 2013.